Molecular Therapy

Preclinical long-lasting efficacy and translational significance of AAV-CaV3.2iPA sensory neuron-targeted analgesia in neuropathic pain

--Manuscript Draft--

Manuscript Number:	
Full Title:	Preclinical long-lasting efficacy and translational significance of AAV-CaV3.2iPA sensory neuron-targeted analgesia in neuropathic pain
Article Type:	Research Article
Keywords:	Molecular therapy; Chronic pain; Primary sensory neurons; Adeno-associated virus; Calcium channel 3.2 (CaV3.2); Inhibitory peptide aptamer
Corresponding Author:	Hongwei Yu Medical College of Wisconsin Milwaukee, UNITED STATES
First Author:	Seung Min Shin, PhD
Order of Authors:	Seung Min Shin, PhD
	Brandon Itson-Zoske
	Fan Fan, MD
	Quinn H. Hogan, MD
	Hongwei Yu, MD
Abstract:	We recently reported that targeting intrinsically disordered regions of calcium channel 3.2 (CaV3.2) facilitated the discovery of potent CaV3.2 inhibitory peptide aptamers (3.2iPA1 and 2) for AAV-mediated peripheral sensory neuron-targeted analgesia in rat chronic pain models. However, the preclinical long-term efficacy of the approach and the translational significance of 3.2iPAs in blocking T-type/CaV3.2 in human sensory neurons are not established. In this report, we generated AAV6.2FF-encoded concatemeric 3.2iPA (Co3.2iPA) that combines 3.2iPA1 and 2 as a tandem repeat. We tested its effectiveness via injection of AAV6.2FF-Co3.2iPA into the pathological dorsal root ganglia and evaluated analgesic efficacy in relieving stimulated and spontaneous pain behaviors lasting up to 3.5 months in rat Tibial Nerve Injury (TNI)-induced painful neuropathy. Results showed that AAV6.2FF-Co3.2iPA treatment produced analgesic effects that were comparable between male and female rats in magnitude and time course. Immunohistochemistry and AAV genome analysis confirmed peripheral nerve-restricted AAV6.2FF-Co3.2iPA biodistribution and long-term transgene expression. Inhibition of T-type/CaV3.2 channels and suppression of action potential firing by expressing Co3.2iPA was demonstrated in the human induced pluripotent stem cells-derived sensory neurons (hiPSC-SNs), suggesting a translational potential of sensory neuron-targeted AAV6.2FF-Co3.2iPA treatment for clinical chronic pain conditions that are intractable to currently available pain therapy.
Suggested Reviewers:	Fletcher A. White, PhD Professor, Indiana University Purdue University Indianapolis fawhite@iupui.edu Pain Scientist
	Gerald W Zamponi, PhD Professor, University of Calgary zamponi@ucalgary.ca Pain research Scientist
	Sascha R.A. Alles, PhD Assistant professor, University of New Mexico salles@salud.unm.edu Pain Scientist
Opposed Reviewers:	

Powered by Editorial Manager® and ProduXion Manager® from Aries Systems Corporation

Cover letter

Hongwei Yu, M.D.
Professor

MEDICAL COLLEGE OF WISCONSIN

Department of Anesthesiology

August 25, 2024
Dr. Roland Herzog
EDITOR-IN-CHIEF
Molecular Therapy

RE: Preclinical long-lasting efficacy and translational significance of AAV-Ca_V3.2iPA sensory neuron-targeted analgesia in neuropathic pain

Dear Dr. Herzog:

We are submitting an original research article entitled “Preclinical long-lasting efficacy and translational significance of AAV-Ca_V3.2iPA sensory neuron-targeted analgesia in neuropathic pain” for your consideration of publication in Molecular Therapy.

We reported[1,2] that targeting intrinsically disordered regions of calcium channel 3.2 (Ca_V3.2) facilitated the discovery of potent Ca_V3.2 inhibitory peptide aptamers (3.2iPA1 and 2) for AAV-mediated sensory neuron-targeted analgesia in rat chronic pain models. Translation of this discovery into a practical analgesic approach could enhance addiction-free treatment options for chronic pain. However, the preclinical long-term efficacy of the approach, molecular mechanisms, and the translational significance of 3.2iPAs in blocking T-type/Ca_V3.2 in human sensory neurons have not been established. Significant new findings supplemental to our previous reports include: 1) AAV6.2FF-mediated concatemeric 3.2iPA (Co3.2iPA that combines 3.2iPA1 and 2, both exhibiting comparable Ca_V3.2 inhibition and analgesic potent in chronic pain models) expression lasts long-term (3.5 months), restricted in PSNs and peripheral sensory pathways after DRG delivery. This results in long-lasting analgesic success in both male and female rats subjected to tibial nerve injury-induced neuropathic pain. 2) Co3.2iPA expression results in selective T-channel inhibition and suppression of AP firing of the human induced pluripotent stem cells-derived sensory neurons (hiPSC-SNs), suggesting a translational potential.

This article has not been submitted for publication, nor has it been published as a whole elsewhere, including on the Internet. An abstract has been accepted for oral presentation in the 2024 SFN Chicago meeting (Oct 5-9, 2024). I attest that all authors listed on the title page have read and approved the manuscript, attested to the validity and legitimacy of the data and its interpretation, and agreed to its submission to Molecular Therapy. The authors declare that they have no competing interests.

Sincerely
Hongwei Yu

Hongwei Yu, MD
Professor, Anesthesiology
Member, Neuroscience Research Center

Department of Anesthesiology
Medical College of Wisconsin
8701 Watertown Plank Road
Milwaukee, Wisconsin 53226
Tel: (414) 955-5745, Fax: (414)955-6507
e-mail: hyu@mcw.edu

References

1 Itson-Zoske, B., Shin, S. M., Xu, H., Qiu, C., Fan, F., Hogan, Q. H. *et al.* Selective block of sensory neuronal T-type/Cav3.2 activity mitigates neuropathic pain behavior in a rat model of osteoarthritis pain. *Arthritis Res Ther* **24**, 168, doi:10.1186/s13075-022-02856-0 (2022).

2 Shin, S. M., Lauzadis, J., Itson-Zoske, B., Cai, Y., Fan, F., Natarajan, G. K. *et al.* Targeting intrinsically disordered regions facilitates discovery of calcium channels 3.2 inhibitory peptides for adeno-associated virus-mediated peripheral analgesia. *Pain* **163**, 2466-2484, doi:10.1097/j.pain.0000000000002650 (2022).

Manuscript (including text, tables and captions)

Click here to view linked References

Click here to access/download;Manuscript (including text, tables and captions);Manuscript MT.docx

Preclinical long-lasting efficacy and translational significance of AAV-Cav3.2iPA sensory neuron-targeted analgesia in neuropathic pain

Seung Min Shin[a¶], Brandon Itson-Zoske[a¶], Fan Fan[c], Quinn H. Hogan[a], and Hongwei Yu[a*]

[a] Department of Anesthesiology, Medical College of Wisconsin, Milwaukee, WI 53226

[c] Department of Physiology, Medical College of Georgia, Augusta University, Augusta, GA 30912

[*] Correspondence should be addressed to Hongwei Yu, Email: hyu@mcw.edu, Phone: 414-955-5745, Fax: 414-955-6507.

[¶] These authors contributed to this work equally

Abstract

We recently reported that targeting intrinsically disordered regions of calcium channel 3.2 ($Ca_V3.2$) facilitated the discovery of potent $Ca_V3.2$ inhibitory peptide aptamers (3.2iPA1 and 2) for AAV-mediated peripheral sensory neuron-targeted analgesia in rat chronic pain models. However, the preclinical long-term efficacy of the approach and the translational significance of 3.2iPAs in blocking T-type/$Ca_V3.2$ in human sensory neurons are not established. In this report, we generated AAV6.2FF-encoded concatemeric 3.2iPA (Co3.2iPA) that combines 3.2iPA1 and 2 as a tandem repeat. We tested its effectiveness via injection of AAV6.2FF-Co3.2iPA into the pathological dorsal root ganglia and evaluated analgesic efficacy in relieving stimulated and spontaneous pain behaviors lasting up to 3.5 months in rat Tibial Nerve Injury (TNI)-induced painful neuropathy. Results showed that AAV6.2FF-Co3.2iPA treatment produced analgesic effects that were comparable between male and female rats in magnitude and time course. Immunohistochemistry and AAV genome analysis confirmed peripheral nerve-restricted AAV6.2FF-Co3.2iPA biodistribution and long-term transgene expression. Inhibition of T-type/$Ca_V3.2$ channels and suppression of action potential firing by expressing Co3.2iPA was demonstrated in the human induced pluripotent stem cells-derived sensory neurons (hiPSC-SNs), suggesting a translational potential of sensory neuron-targeted AAV6.2FF-Co3.2iPA treatment for clinical chronic pain conditions that are intractable to currently available pain therapy.

Introduction

Chronic neuropathic pain is a critical treatment challenge.[1,2] Although the central nervous system (CNS) is required for conscious pain perception, hyperexcitability of peripheral sensory neurons (PSN) induced by nerve injury in the peripheral somatosensory nervous system is sufficient and necessary to initiate and maintain neuropathic pain.[3] Clinical chronic pain in almost all cases is maintained by ongoing afferent hyperactivity originating from peripheral pathological sources.[4-6] Therefore, treatments targeting the PSNs will be devoid of CNS adverse effects and are most likely to succeed.[5,7]

Up-regulation of peripheral sensory neuronal calcium channel 3.2 ($Ca_V3.2$) is a common feature and a major molecular driver in the pathogenesis of multiple pain conditions in preclinical models [8-10] and human pain.[11,12] Our previous studies showed that PSN-specific block of T-type/$Ca_V3.2$ by AAV-encoded $Ca_V3.2$ inhibitory peptide aptamer (3.2iPAs) has clear analgesic effects in mitigation of established pain behaviors of rat chronic pain models.[13,14] Results implicate the potential of this approach to be developed as a safe, abuse-free clinical pain therapy for intractable pain conditions that can't be controlled with standard medical care. Many challenges, as well as opportunities, remain for carrying this project forward. For example, 1) Will AAV-encoded 3.2iPA be expressed persistently in the peripheral sensory pathway after dorsal root ganglia (DRG) delivery, thereby eliciting long-lasting analgesic success? 2) Biological differences in sensory processing between human and model organisms may present significant obstacles to translational approaches in treating chronic pain.[15,16] Does T-channel inhibition by 3.2iPA represent a meaningful index of the analgesic therapeutics in human sensory neurons? These challenges must be met as we pursue the opportunity to carry this sensory neuron-specific 3.2iPA-analgesia for clinical chronic pain therapy.

A human sensory neuron model is necessary for the development of new and more effective analgesics. Since human DRG sensory neurons are not readily available from living donors for ethic and logistic reasons, human induced pluripotent stem cell-derived sensory neurons (hiPSC-SNs) provide valuable opportunities in pain research and medicine development.[17-19] Many hiPSC-SNs differentiation protocols have been established recently, and well-defined hiPSC-SNs are commercialized with scalable and fully automated protocols to generate pure cultures of sensory neurons in large quantities under chemically defined conditions.[20,21] Studying hiPSC-SNs can avoid species differences and mitigate failures in translation, leveraging our basic research findings to improve translational success.

Two $Ca_V3.2$iPAs (3.2iPA1 and 2) were defined in our previous studies as selective $Ca_V3.2$ inhibitors with comparable in vivo analgesic potent.[13,14] In this report, we generated AAV6.2FF-encoded concatemeric 3.2iPA (Co3.2iPA) that combines 3.2iPA1 and 2 as a tandem repeat. We expanded treatment duration up to three and half months after DRG delivery of AAV6.2FF-Co3.2iPA in both male and female rats with TNI-induced painful neuropathy, and analgesic effects on both stimulated and spontaneous pain behaviors were evaluated. AAV6.2FF-Co3.2iPA in vivo biodistribution along the peripheral sensory pathway and off-side tissues and long-term transgene expression were analyzed by immunohistochemistry and quantitative PCR (qPCR) of AAV genome copy numbers. The translational significance of Co3.2iPA for inhibition of T-channels and action potential generation was determined using hiPSC-SNs as a leveraging human sensory neuron model.

Results

Long-lasting analgesia after DRG treatment by AAV6.2FF-Co3.2iPA in male rats

Experimental design. In this study, a concatemeric 3.2iPA that combines 3.2iPA1 and 3.2iPA2[13] (Co3.2iPA, GFP-fusion) was constructed for enhancement of 3.2iPA target engagement and $Ca_V3.2$-blocking efficacy. Triple glycine (G) was inserted between 3.2iPA1 and 3.2iPA2 for stabilizing complex[22] and the transgene was transcribed by a hybrid CMV enhancer/chicken β-actin (CBA) promoter. A GFP-fused 2 copies of 3.2NP (Co3.2NP), which is a non-functional peptide from $Ca_V3.2$ N-terminus,[13] was constructed as the control. Whole-cell patch-clamp recording of HEK cells with stable expression of human $Ca_V3.2$ (HEK3.2) transfected with the plasmid encoding Co3.2iPA confirmed that Co3.2iPA inhibited $Ca_V3.2$ conductance >50% of naïve HEK3.2 cells, while no effect was observed in presence of Co3.2NP (**Figure 1**). AAVs were packed into serotype 6.2FF, which is a triple AAV6 variant containing F129L, Y445F, and Y731F mutations and shows more rapid and potent in vivo transduction than AAV6.[23] Throughout the results of this manuscript, we used 'Co3.2iPA' as the treatment vector and 'Cop' as the control, respectively.

Since sex differences exist in experimental and clinical pain and in the responsiveness to treatment, [24] pain hypersensitivity and pain reversal responses to treatment were examined in both male and female rats for this study. In the behavior experimental design, the sensitivity to mechanical and thermal hindpaw cutaneous stimulation was assessed at baseline (BL) and weekly after TNI induction for 2 weeks before DRG injection of AAVs. Rats were then randomized to receive intraganglionic injection of either AAV6.2FF-Co3.2iPA or AAV6.2FF-CoNP into the L4/L5 DRG

ipsilateral to Tibial Nerve Injury (TNI), after which sensory behaviors were evaluated for 3.5 months. The presence of spontaneous pain was determined by gabapentin (GBP,100mg/kg, i.p.)-induced conditioned place preference (CPP) test in both groups as a terminal experiment to evaluate spontaneous pain-associated behaviors, as we described previously.[25,26] Behaviors measured before vector injection on the 14th day after TNI, a time-point of hypersensitization is fully established,[13] were used as treatment baseline (tBL) to evaluate the effectiveness and % of hypersensitivity reduction after AAV treatment (**Figure 2A-B)**. After behavior evaluation processes, animals were euthanized, and tissues were harvested for AAV genome analysis by quantitative polymerase chain reaction (qPCR) and GFPCo3.2iPA transduction in DRG by immunohistochemistry (IHC).

Behavior evaluation. Results showed that all tested rats established multiple modalities of evoked pain behaviors 2 weeks after TNI, including hypersensitivity to mild mechanical stimuli (vF testing), more frequent hyperalgesic-type responses (sustained lifting, shaking, and grooming) after noxious mechanical stimulation (Pin testing), and hypersensitivity to heat and cooling (acetone) stimulation. These behaviors persisted after injection of the control AAV6.2FF-CoNP during the 3.5 months of the observation course. In contrast, rats injected with AAV6.2FF-Co3.2iPA showed a reversal of these changes, which persisted throughout the observation period and potentially outlasted (**Figure 2C-F**). A typical requirement for a 'minimum clinically important difference' in analgesic trials is ≥30% or more of pain reduction.[27-30] Since the pain hypersensitivity in multiple modalities was fully established 2 weeks after TNI as we reported in the previous reports,[13,26,31] we specified the measures on the 14th day after TNI and before AAV treatment (tBL) as the peak pain intensity (100%), and the measures of each sensory modality after

treatment were normalized to the measures at the tBL and presented as the percentage of pain relief for each modality at each time point thereafter (**Figure 2C1-F1**). The average pain relief in the 3.5-month treatment course showed 52%, 49%, 69%, and 67% reduction of vF-, Pin-, Cold-, and Heat-stimulated mechanical and thermal pain behaviors, respectively (**Figure 2G)**. Using a biased CPP paradigm,[13,14] the effect of AAV6.2FF-Co3.2iPA treatment on the affective aspects of spontaneous pain was evaluated. None of the animals in either group were excluded from the study because of their baseline preference/avoidance for a chamber. A significant conditioning effect of GBP administration was observed in the TNI rats injected with AAV6.2FF-Co3.2iPA, while there was no significant difference in the time spent in the initially nonpreferred chamber during baseline vs. testing period in AAV6.2FF-CoNP-injected TNI animals, indicating that AAV6.2FF-Co3.2iPA treatment relieves on-going spontaneous pain in TNI rats (**Figure 2H)**.

In vivo sensory neuron transduction. IHC was performed to determine the in vivo transduction rate for AAV6.2FF-Co3.2iPA after behavior evaluation (**Figure 3**). The Co3.2iPA-positive neurons (GFP) comprised 50 ± 6%, ranging 23~81% (1275 out of 2827 total neuronal profiles) identified by pan-neuronal marker β3-tubulin (n = 3 DRG, 3-4 sections per DRG, selected as every fifth section from the consecutive serial sections). Colocalization double immunostaining with markers, including pan-neuronal β3-tubulin (Tubb3), $Ca_V3.2$, isolectin-IB4 and calcitonin gene-related peptide (CGRP) for C and Aδ sensory neurons, sodium/potassium ATPase 1 alpha (NKA1α) for neuronal plasma membrane (PM), NeuN for neuronal nuclei, and glial fibrillary acidic protein (GFAP) for perineuronal glia. The results showed that Co3.2iPA was preferably transduced to sensory neurons, including the full-size range of the PSNs that also expressed $Ca_V3.2$. The expression profile revealed multiple subcellular localizations, preferably in the PSN cytosol,

nucleus, and plasma membrane, but not in the perineuronal glial cells, as we have reported previously for individual 3.2iPA.[13]

QPCR AAV genome. The positive amplification of AAV genome was defined as the samples (naïve rats) with copy numbers greater than average (180 copies) plus 3 standard deviations (99 copies). Therefore, the limit of quantification[32] (Loom, the lowest number of copies that can be reliably measured) was set at 500 copies as the cutoff value in the presence of 2 ng of total DNA for this study. Samples of total DNA from tissues, CSF, and sera from AAV6.2FF-Co3.2iPA (n=6) were evaluated for the presence of AAV genomes. AAV6.2FF-Co3.2iPA qPCR analysis on the DNA samples extracted from multiple tissues after behavior evaluation in male animals showed that the AAV genomes were detected in all L4 (6) and L5 (6) DRG ipsilateral to AAV6.2FF-Co3.2iPA treatment from 6 rats, as well as the lumbar spinal cords, at 3.5 months after AAV6.2FF-Co3.2iPA injection, confirming that the pathological DRG did receive the AAV and persistent transgene expression. There were low positive signals in the two contralateral DRG at marginally higher than 500 copies of the AAV6.2FF-Co3.2iPA genome. AAV genome amplification showed lower than cutoff value in the sciatic nerve ipsilateral to AAV injection and in the tissues of the brain cortex, heart, liver, kidney, and biofluids (blood and CSF) in the animals subjected to intraganglionic injection of AAV6.2FF-Co3.2iPA (**Figure 4**). These results suggest that the AAV6.2FF-Co3.2iPA persists in the injected DRG for the long term.

These findings together demonstrate that DRG injection of AAV6.2FF-Co3.2iPA induces long-term Co3.2iPA expression, restricted to the PSNs of injected DRG and their peripheral and central afferents. This strategy via AAV-mediated expression of Co3.2iPA targeted to sensory neurons in

178 the anatomically segmental sensory ganglia responsible for pain pathophysiology has clear, long-
179 lasting analgesic effectiveness in normalizing the established peripheral hypersensitivity for both
180 evoked and spontaneous pain behaviors in TNI-induced painful neuropathy.
181
182 **Analgesia of DRG-AAV6.2FF-Co3.2iPA treatment in female TNI rats**
183 A treatment protocol in female TNI rats was conducted similarly to the tests in male animals, as
184 described in Figure 2. Results showed that the female rats displayed comparable phenotypic
185 development of hypersensitivity after induction of TNI to male rats and that both evoked
186 mechanical/thermal hypersensitivity and GBP-CPP responses were normalized in the 3.5 months
187 of observation course after AAV6.2FF-Co3.2iPA treatment, showing comparable analgesic effects
188 to the male animals (**Figure 5A-F**). The average reversal of TNI-induced hypersensitivity on vF-,
189 Pin-, Cold-, and Heat-stimulated mechanical and thermal pain behaviors in the 3.5-month
190 treatment course was 53%, 49%, 59%, and 70%, respectively. Thus, a sexual dimorphism seems
191 not apparent for both pain behavior phenotypes after TNI and in responsivity to DRG-AAV6.2FF-
192 Co3.2iPA treatment. IHC on the DRG sections from female TNI rats after behavior evaluation
193 revealed a GFPCo3.2iPA expression profile with Co3.2iPA-positive neurons comprising 52 ± 6%
194 of in vivo transduction rate (17~80%, 1284 out of 2665 total Tubb3-positive neurons) (**Figure 5G**).
195
196 **Initial testing of Co3.2 iPA molecular mechanisms**
197 **Cav3.2iPA interaction with full-length Cav3.2 protein**. Previous reports found that 3.2iPA1 and
198 3.2iPA2 displayed similar inhibitory effects on $I_{Ca3.2}$ and comparable potent analgesic effects.[13] We
199 further determined and compared the cellular localization of 3.2iPA1 and 3.2iPA2 by transfection
200 of individual GFP3.2iPA1 and GFP3.2iPA2 into HEK cells, followed by immunoblots on extracted

cytosol, membrane, and nuclear samples. Results showed multiple localization of both GFP3.2iPA1 and GFP3.2iPA2 in the cytosol, membrane, and nuclear fractions (**Figure 6A**). Studies report that intracellular intrinsically disordered regions (IDRs) of membrane proteins are favorable for reversible low-to-moderate-affinity engagement in interactions with the membrane.[33] To test whether 3.2iPA1 and 2 interference of $Ca_V3.2$ function might be via direct binding to full-length $Ca_V3.2$, GFP affinity pull-down by ChromoTek GFP-Trap (ChromoTek, Rosemont, IL) was performed after transfection of GFP3.2iPA1 and GFP3.2iPA2 in HEK3.2 cells using GFP and GFP-NP as the controls. Cell lysates were prepared by a lysis buffer containing 0.5% Nonidet p40, a 'non-denaturing' mild lysis detergent, for preventing interaction breaking and maximizing the retention of 3.2iPA-protein interactions.[26,34] Immunoblots detected full-length $Ca_V3.2$ protein trapped in both GFP3.2iPA1 and GFP3.2iPA2 pull-down samples but not in controls (**Figure 6B**, **C**). The gel pieces of controls (pooled GFP and GFPNP) and 3.2iPAs (pooled GFP-3.2iPA1 and 2) around 180-300kDa from the silver-stained gel (**Figure 6B)** were excised for mass spectrometry. Results of nano reversed-phase liquid chromatography tandem mass spectrometry (nLC-MS/MS) showed MS/MS spectra of ions matching unique human $Ca_V3.2$ peptides (**Figure 6D** and **Table 1**), confirming $Ca_V3.2$ in the 3.2iPA1/2 pull-down samples. Since 3.2iPAs show an absence of pleiotropic effects on other ion channels,[13] these results suggest that the 3.2iPA1 and 2 blocking of $Ca_V3.2$ channel activation is by selective binding to the $Ca_V3.2$ protein, perhaps through an undefined intra-molecular domain-domain interaction (intraDDI) that needs further investigation.[35]

Co3.2iPA binding to phospholipids. Membrane lipids are important regulators of calcium channel activity,[36] and polybasic IDRs in transmembrane proteins preferably bind to negatively

charged lipids via electrostatic interactions.[37,38] We therefore reasoned that 3.2iPA (1/2) may be able to bind phosphoinositides. This hypothesis was tested by using phosphatidylinositol phosphate (PIP) strips (Echelon PIP Strip, Salt Lake City, UT), as described previously,[26] and GFP-Co3.2iPA and GFP-Cop (control) were used for testing. Specifically, GFP-Co3.2iPA and GFP-cop were transfected into neuronal Neuro-2A cells for 48 hr, and cell lysates were prepared by a RIPA buffer containing 0.1% SDS and 1% Triton X100 (strong detergents) and 1% deoxycholate (anionic detergent) for maximally denaturing to break Co3.2iPA interaction complex formations.[26] Silver stain after SDS-PAGE gel showed clean purification of GFPCoNP and GFPCo3.2iPA (**Figure 6E)** and the purified samples were applied to the PIP strips. Results showed that purified GFPCo3.2iPA was efficiently bound to several anionic PIPs and phosphatidylserine (PS) (**Figure 6F)**. In contrast, the affinity pull-down GFPCoNP did not show clear binding to lipid spots as previously reported.[26,39] These findings are consistent with the reports that basic residues, often clustered in IDRs, can modulate membrane protein functions by binding to the membrane via electrostatic interactions with lipids.[40,41]

Impact of Co3.2iPA on T-channel electrogenesis of hiPSC-SNs

Characterization of hiPSC-SN differentiation and LV transduction. Biological differences in sensory processing by T-channels between human and animal models may present significant obstacles to translational approaches in treating chronic pain. To leverage our basic findings for improving translational success, we next investigated the expression of Co3.2iPA on ionic channel electrogenesis in hiPSC-SNs (female, Anatomic, Minneapolis, MN).[21] The hiPSC-SNs were developed from female human neural crest stem cells. Our initial characterization showed that hiPSC-SNs were differentiated to small-sized PSN morphology with a soma diameter around

20~25μm and developed extensive neurites after Days In Vitro (DIV) 4-7, indicating that these cells were efficiently committed to the neuronal lineage. $Ca_V3.2$ protein ($Ca_V3.2$ antibody is validated [13,42]), $Ca_V2.2$, and Sodium channel 1.7 were expressed by immunocytochemistry (ICC) tests. T-type/$Ca_V3.2$ current (LVA I_{Ca}), high-voltage gated calcium channels (HVA I_{Ca}), tetrodotoxin-sensitive and resistance (TTXs and TTXr) I_{Na}, and induction of action potentials were ready to be recorded at DIV21 (**Figure S1A-H**). Results indicate that hiPSC-SNs are maturing differentiation, reproduce several key electrophysiological properties expected from bona fide DRG sensory neurons, and are useful for supporting drug discovery programs for pain.

We next established a lentivector (LV) protocol to efficiently transduce transgene into the cultured hiPSC-SNs. Overall, the LV multiplicity of infection (MOI) of 5 appeared sufficient to allow clear visualization of GFP in nearly 100% transduction with extensive neurite outgrowth. This indicates no apparent cellular toxicity in our cultural condition since live-cell imaging of neurite outgrowth can be used for evaluating neurotoxicity.[43] GFP signals were visualized at DIV2-3 after the addition of LV-GFP, showing that the GFP signal increased as a function of the MOI and the time after transduction, with intensity increase over several days and persistence in DIV35 of observation.

Co3.2iPA selective inhibition of T-channels in hiPSC-SNs. We generated LV-Co3.2iPA and LV-CoNP (**Figure S2**) and hiPSC-SNs were cultured in differentiation conditions for DIV21 before LVs transduction at MOI≈5. GFP-fused CoNP and Co3.2iPA expression were observed in nearly 100% of hiPSC-SNs 4 days after adding LVs. At DIV26, hiPSC-SNs were collected, and the cytosol, membrane, and nuclear samples were extracted to determine Co3.2iPA cellular

localization by immunoblots. Results revealed that CoNP was detected only in the cytosol, but Co3.2iPA was detected in the extracted cytosol, membrane, and nuclear samples. Endogenous full-length $Ca_V3.2$ was enriched in the hiPSC-SN membrane, while $Ca_V3.2$ was detected in both membrane and nuclear fractions of Co3.2iPA-expressing hiPSC-SNs (**Figure 7A-C**). ICC image of $Ca_V3.2$ expression in hiPSC-SNs showed diffuse cytoplasmic staining but absence of $Ca_V3.2$ accumulation within the nuclei of the cultured hiPSC-SNs (**Figure S1B**), suggesting that $Ca_V3.2$ detection upon immunoblot in extracted nuclear samples likely reflected $Ca_V3.2$ associated perinuclear components.[44,45] Whole-cell patch-clamp recordings showed that Co3.2iPA expression significantly inhibited T-channel currents and suppressed action potential firing frequency, compared to naïve and CoNP-expressing hiPSC-SNs (**Figure 7D-M**). To test whether Co3.2iPA expression will have pleiotropic effects on the other ion channel conductance, we recorded HVA I_{Ca}, total and TTXs/TTXr I_{Nas}, and BK potassium channels (BK I_{KV}). These data showed that LVA I_{Ca} inhibition was selective since Co3.2iPA expression did not affect HVA I_{Ca}, TTXs/TTXr I_{Na}, and BK I_{KV} channel conductance (**Figure S3**). Since the electrostatic interaction between polybasic domains of peripheral proteins and anionic lipids is generally nonspecific,[46] our results cannot rule out the possibility that Co3.2iPA may bind to other unknown targets. Together, the data afford a likely mechanism that, as a polybasic-enriched peptide, Co3.2iPA inhibits $Ca_V3.2$ conductance due to direct binding to membrane $Ca_V3.2$ via an electrostatic mechanism or $Ca_V3.2$ intramolecular domain-domain interaction.[35,47] This resembles the reports that show the interaction of $Ca_V3.2$ intracellular loop (ICL) peptide with $Ca_V3.2$ protein.[48] An intracellular polybasic motif is required for channel function and plasma membrane binding of the polybasic motif in the I-II linker stabilizes voltage-gated $Ca_V1.2$ channel function.[38] Future studies will investigate Co3.2iPA membrane-targeting mechanisms.

Discussion

$Ca_V3.2$ in PSNs is a crucial pain mediator and has been targeted for developing analgesics for its role in pain.[8,9] However, an effective, peripherally targeted, safe analgesic approach targeting PSN-$Ca_V3.2$ without addiction risk for treating chronic pain is still clinically unavailable. The new findings of this study supplementing our previous reports[13,14] include that 1) AAV6.2FF-mediated Co3.2iPA expression lasts long-term in PSNs after DRG delivery and provides long-lasting analgesia in relief of neuropathic pain; 2) Co3.2iPA expression results in selective T-channel inhibition and suppression of AP firing of the hiPSC-SNs, supporting a translational potential; and 3) Although the AAV capsid-specific humoral immunity was not examined in this study, long-term Co3.2iPA expression and AAV genome presence in the injected DRG suggest tolerable immunogenicity against AAV6.2FF-Co3.2iPA, which can limit the duration of transgene expression.[49,50] It is reported that rats exhibit the lowest levels of AAV6 neutral antibody compared to other species, [51] and AAV6.2FF displays higher resistance to pooled immunoglobulin neutralization and mediates long-term transgene expression in vivo.[23,52] Long-term AAV-medicated transgene expression is observed in quiescent neurons,[53] including AAV pain therapy.[54] Clinical trial suggests that AAV vector immunogenicity is dose-dependent.[55] These imply that small AAV6.2FF-Co3.2iPA doses for DRG injection and restricted PSN expression will not result in a significant immune response that would otherwise induce loss of transgene expression. Additionally, Co3.2iPA inhibits T-channels of hiPSC-SNs cultured in vendor-defined high glucose (17.5mM) media, suggesting the potential efficacy of Co3.2iPA in diabetic pain.

315 Reversing the afferent hyperexcitability due to ion channel dysfunction induced by peripheral
316 nerve damage is an emerging target for pain therapy.[5,9,56] DRG primary sensory neurons are
317 promising targets for developing peripheral analgesic strategies for chronic pain treatment due to
318 their key role in pain etiology, accessible anatomical location, and the potential for different pain
319 hub interventions. PSNs represent a 'low-hanging target' in the development of safe therapies for
320 patients with chronic pain.[5,7] Delivering drugs to the DRG is well-developed and safe, for instance,
321 as used by anesthesiologists for regional blockade and by pain physicians for diagnosis and
322 treatment of radiculopathy.[57] Injection into the DRG has minimal consequences in preclinical
323 models.[58] Unintentional intra-ganglion injection commonly accompanies clinical transforaminal
324 epidural steroid injection, a very common procedure with minimal risk of nerve damage.[57] Thus,
325 the PSNs are particularly suitable for targeting new analgesic treatments, especially at the levels
326 of associated pathological DRG.[59,60] Our and other studies show that targeting ectopic nociceptive
327 signals emanating from injured DRG neurons can provide effective analgesia by blocking action
328 potentials that cause or maintain the chronic pain state.[13,26,31,61,62]
329
330 It is reported that central nervous system gene therapy by intravenous high-dose AAV causes
331 asymptomatic and self-limited DRG inflammation and mild PSN degeneration in primates.[63-65]
332 Since these changes are very minor in comparison to those induced by painful neuropathic
333 conditions that AAV injection would treat, this is unlikely to become a barrier to the clinical
334 application of our approach. In preclinical models, direct DRG delivery of AAVs encoding
335 analgesic biologics targeting dysfunctional pronociceptive molecules can relieve chronic pain,
336 flexibility for selective segmental localization, and minimal behavior changes attributable to the
337 surgical procedure.[66] Recently, injection techniques have been advanced to achieve minimal

338 invasive delivery of biologics for future clinical pain therapy. [67,68] The feasibility and safety of
339 injection into human DRGs are clearly demonstrated by clinical experience [57] , and DRG delivery
340 of pain medicine is being applied to treat human pain.[69]
341
342 The present study and our previous reports [13,14] show that, on average, 30-50% in vivo selective
343 sensory neuron transduction by AAV-encoded 3.2iPA (or Co3.2iPA) results in over 50% reduction
344 of mechanical and thermal pain modalities. This suggests that a complete PSN transduction for
345 $Ca_V3.2$ inhibition is not needed to achieve meaningful and substantial pain relief. This may result
346 from several possible mechanisms. Although PSN somata in DRG are anatomically isolated from
347 each other and are not synaptically interconnected, most DRG-PSNs are transiently depolarized or
348 synchronized cluster firing of adjacent DRG neurons when axons of neighboring neurons of the
349 same ganglion are stimulated repetitively.[70,71] This coupling activation occurs among various-sized
350 neurons, including small-diameter nociceptors and large-diameter low-threshold
351 mechanoreceptors.[72] Therefore, although AAV directly transduces only a subpopulation of the
352 sensory neurons, their reduced pronociceptive ion channel activity additionally reduces adjacent
353 non-transduced neuron activity due to this coupling mechanism. Additionally, injury-induced
354 peripheral hypersensitization associated with $Ca_V3.2$ malfunction may affect multiple sites of the
355 peripheral sensory neurons, including impulse generation in the peripheral terminals, enhanced
356 ectopic excitability of the PSN soma, reduced T-junction filtering of AP trains, and elevated
357 neurotransmission in the spinal dorsal horn. Biodistribution of AAV after DRG injection is
358 restricted along the peripheral sensory pathways and spinal dorsal horn, and therefore, pain relief
359 could be also due to channel inhibition in multiple sites. Finally, Both 3.2iPA1 and 3.2iPA2 show
360 significant inhibition of $Ca_V3.1$,[13] which is a pain hub;[73,74] thus, pain relief by Co3.2iPA is

predicted to involve the block of both $Ca_V3.1$ and $Ca_V3.2$. Further study will test the DRG dose of therapeutic AAV-Co3.2iPA and pain behavior attenuation response to determine the minimal and appropriate clinical dose selection of AAV6.2FF-Co3.2iPA for pain relief.

Inclusion, our study demonstrates that AAV6.2FF-encoded Co3.2iPA be selectively expressed in the peripheral sensory pathways for long-term after DRG delivery, providing long-lasting analgesia of neuropathic pain. The AAV6.2FF-mediated durable Co3.2iPA expression and long-term analgesia indicate that approach could provide a viable alternative to the current pain treatments which have led to the opioid crisis, and the results of hiPSC-SNs are significant in leveraging our basic findings to improve translational success. Several limitations in the current study are acknowledged. For example, the efficacy of Co3.2iPA needs to be confirmed in pain modeling human sensory neurons (h-SNs) (when available) since h-SNs contain a variety of sensory neuronal subtypes such as low-threshold mechanoreceptors (LTMRs) and high-threshold mechanoreceptors (HTMRs) with different biological and EP properties, and h-SN culture also contains glial cells, making h-SN advantageous for the holistic study of sensory neurons rather than as single cell type of hiPSC-SNs.[75,76] Moreover, the molecular mechanisms of Co3.2iPA in modulating $Ca_V3.2$ channels need to be further delineated in sensory neurons, which could be critical for the assessment of therapeutic efficacy and potential side effects.

Materials & Methods

Animals and Study Approval

Adult male and female Sprague Dawley (SD) rats weighing 100-125g body weight (Charles River Laboratories, Wilmington, MA) were used. All animal experiments were performed with the approval of the Medical College of Wisconsin Institutional Animal Care and Use Committee (AUA00007371) in accordance with the National Institutes of Health Guidelines for the Care and Use of Laboratory Animals. Animals were housed individually in a room maintained at constant temperature (22±0.5°C) and relative humidity (60±15%) with an alternating 12h light-dark cycle and were access to water and food ad libitum throughout the experiment. All efforts were made to minimize suffering, and all survival surgeries were completed in a sterile environment under a surgical microscope in animals anesthetized with isoflurane (2–5%). For tissue harvest euthanasia, animals were deeply anesthetized by isoflurane followed by decapitation with a well-maintained guillotine. The estimated numbers of animals needed were derived from our previous experience with similar experiments [13] and power analysis was not performed. The numbers of rats used were detailed in the relevant sections or figure legends of the experiments. The uses of AAV and human iPSC sensory neurons were approved by the Medical College of Wisconsin Institutional Biosafety Committee, with approval numbers IBC20140322 and IBC20220103.

Cell culture

Cell lines: HEK293 cells (ATCC), HEK293 cells stably expressing human wide-type $Ca_V3.2$ (HEK3.2, Kerafast Boston, MA), and Neuro-2A cells (N2A, ATCC) were cultured in Dulbecco's

modified Eagle's medium (DMEM) supplemented with glutamax, 10% fetal bovine serum (ThermoFisher, Rockford, IL), and antibiotics using standard techniques.

HiPSC-SNs: HiPSC-SNs, which are derived from female human ectoderm-neural crest stem cells, and ChronoTM Senso-MM complete growth high-glucose (17.5mM) medium were purchased from Anatomic (Minneapolis, MN).[21,77,78] HiPSC-SNs maturing differentiation culture was performed per the manufacturers' recommendation.

Molecular cloning and viral constructs

AAV vectors: The DNA fragment encoding the concatemeric human $Ca_V3.2$iPA1 and $Ca_V3.2$iPA2 in tandem repeat (Co3.2iPA) was synthesized and subcloned into BsrG I/Sal I sites (Genscript, Piscataway, NJ) of a single-strand AAV expressing plasmid pAAV-CBA-GFP to generate pAAV-CBA-GFPCo3.2iPA (pAAV-Co3.2iPA).[13] A plasmid of pAAV-CBA-GFP3.2CoNP (pAAV-CoNP) was constructed as the control.[13] AAV was packed into serotype 6.2FF, and purified and titrated, as we previously reported.[79] Serotype 6.2FF was engineered by mutagenesis (Genscript, Piscataway, NJ) to generate a triple-mutant AAV6 capsid encoding F129L, Y445F, and Y731F point mutations.[23] The titers (GC/mL) of AAV6.2FF-Co3.2iPA and AAV6.2FF-CoNP vectors were 2.45 $x10^{13}$ and 2.64 $x10^{13}$, respectively. The same batches of AAVs were used in all in vivo experiments.

Generation of lentivector expressing Co3.2iPA and CoNP for hiPSC-SNs transduction: Lentiviral (LV) expression plasmid pWPT-GFP [80] was used to express Co3.2iPA and CoNP (control). In brief, DNA sequences encoding Co3.2iPA and CoNP, respectively, were released from AAV shuttle plasmids (see above) by BsrG I/Sal I and inserted into BsrG I/Sal I sites of pWPT-GFP to generate plasmids of pWPT-GFPCo3.2iPA (pWPT-Co3.2iPA) and pWPT-GFPCoNP

(pWPT-CoNP) (Genscript) (**Suppl. Fig. 1**). Lentivectors were packaged using pWPT-Co3.2iPA and pWPT-CoNP with packaging plasmid pCMVdR8.74 and envelop plasmid pVSV-g, concentrated, and products titrated in the range of $1x10^8$ to $1x10^9$ transduction unit/mL, as previously reported.[80] Cultured hiPSC-SNs were infected by LV-Co3.2iPA or LV-CoNP in the presence of 8μg of polybrene (Sigma-Aldrich, St. Louis, MO) per mL at an optimized multiplicity of infection ≈3-10. After infection at 37°C for 24 hours, the medium was replaced. Transduction efficiency was estimated under a fluorescent microscope by calculating the percentage of green cells out of a total of 200 counted cells.

Microinjection of AAV vectors into DRG

AAV vector solution was microinjected into right lumbar (L) 4 and L5 DRG using previously described techniques.[58] Briefly, the surgically exposed intervertebral foramen was minimally enlarged by removal of laminar bone. Injection was performed through a micropipette that was advanced ~100 μm into the ganglion. Rats received L4 and L5 DRG injections of either AAV6.2FF-Co3.2iPA or AAV6.2FF-CoNP (one vector per rat), consisting of 2 μL with adjusted titers containing a total of $2.0\ x10^{10}$ genome viral particles. Injection was performed over a 5-min period using a microprocessor-controlled injector (Nanoliter 2000, World Precision Instruments, Sarasota, FL, USA). Removal of the pipette was delayed for an additional 5 min to minimize the extrusion of the injectate. Following the injection and closure of overlying muscle and skin, the animals were returned to their housing where they remained as the designed experiments required.

Animal pain model and behavior testing

Tibial nerve injury (TNI). To model clinical traumatic painful peripheral neuropathy, we

449 performed a TNI, an established model of peripheral nerve injury.[81] Animals were anesthetized
450 using isoflurane at 4% for induction and 2% for maintenance. Under anesthesia, the right sciatic
451 nerve was exposed under aseptic surgical conditions by blunt dissection of the femoral biceps
452 muscle. The sciatic nerve and its three branches (sural, common peroneal, and tibial nerves) were
453 isolated. The tibial nerve was then tightly ligated and transected distal to the ligation. The overlying
454 muscle and skin were then sutured following surgery. Sham-operated rats were subjected to all
455 preceding procedures without nerve ligation and transection.
456
457 **Stimulated behavior testing**. Behavioral tests were conducted between 9:00 AM and 12:00 PM,
458 as we described previously.[13,58] In brief, experimenters were blinded to the treatment during all
459 data acquisition. Animals were acclimatized to the test chambers for at least one hour before each
460 test. Stimuli were applied to the lateral margin of the plantar aspect of the foot in the sural area of
461 innervation. Sensory tests included eliciting reflexive behaviors induced at threshold intensity
462 punctate mechanical stimulation (von Frey test), noxious mechanical stimulation (pin), cold
463 stimulation (acetone), and heat stimulation (Hargreaves test), and were carried out as previously
464 described.[58]
465
466 **Gabapentin injection**. Gabapentin (GBP, Sigma-Aldrich) was dissolved in saline immediately
467 before injections and administered intraperitoneally (i.p.) at a volume of 0.5-1.0 ml (final
468 dose=100 mg/kg body weight).
469
470 **Conditioned place preference (CPP)**. The ongoing aversiveness (i.e., the affective dimension of
471 spontaneous pain) was determined by the GBP-induced CPP test, as described previously.[13,14,82] A

3-chamber CPP apparatus was used (Med Associates, St. Albans, VT) in which 2 sliding doors separate the central chamber from the 2 side chambers that have distinct wall stripes and flooring. Animal movement and times spent in each chamber were measured using computer-interfaced infrared photo beams. The CPP procedure consisted of the following phases. 1) On day 1, rats were acclimated to the CPP boxes for 30 min, with open access to each of the three chambers. On the preconditioning day, rats were placed in the grey middle chamber and allowed to explore both sides of the chambers for 15 minutes. the time spent on each side was recorded, and the preferred and nonpreferred chambers were identified. Animals that showed an extremely predetermined level of preference for one chamber (≥70% of total time) at this stage were excluded from further study. 2) On the conditioning days, place conditioning was conducted using a biased assignment approach to drug pairing: saline was paired with the preferred chamber in the morning, and GBP was paired with the non-preferred chamber in the afternoon with a 6 hr interval (injections were never paired with the middle grey chamber). Conditioning consisted of the following sequential steps: intraperitoneal injection and restriction of the animal within the preferred chamber (saline) or non-preferred chamber (GBP) for 45 min. We used a 45-minute conditioning time based on tests that gabapentin maximally reduced mechanical hypersensitivity at 30–60 min after i.p. injection.[13] Animals were conditioned for 2 days since 2-day GBP has been reported sufficient to produce CPP in rodent pain models.[83,84] 3) For postconditioning testing, the animals were placed back into the middle grey chamber of the CPP chambers with free access to all chambers for 15 minutes. The difference score for each animal was calculated by subtracting the time spent in the saline-paired or GBP-paired chamber before pairing (during preconditioning) from the time spent in each chamber after pairing (postconditioning) and then averaged within each group. Each rat had only

494 a single CPP test 3.5 months after AAV injection. A CPP is defined if the animals spend
495 significantly more time in the GBP-paired chamber versus the saline-paired compartment.
496
497 **Cerebrospinal fluid (CSF), blood, and tissue harvest.**
498 Cerebrospinal fluid was collected from the animals, as we described previously.[85] In brief, under
499 isoflurane anesthesia, an incision was made on the back of the neck, and the muscles were
500 separated by blunt dissection. The spinal dura at the atlanto-occipital level was exposed, the
501 cisterna magna was entered with a 27-G needle, and an average of 20 μl of CSF was collected.
502 Animals were euthanized by decapitation for whole blood and tissue harvest after CSF. Tissues
503 harvested include ipsilateral and contralateral L4-L5 DRG, sciatic nerve, lumbar spinal cord, brain
504 cortex, liver, kidney, and heart. After collection of the whole blood, allow the blood to clot by
505 leaving it undisturbed at room temperature for 10 min. Serum was collected after removing the
506 clot by centrifuging at 2,000 x g for 10 minutes in a refrigerated centrifuge. CSF, serum, and tissue
507 samples collected were frozen and stored at −80°C until use.
508
509 **Immunofluorescent staining**
510 Antibody immunoreactions on tissue sections were performed essentially as described
511 previously.[13,80] For immunocytochemistry (ICC), cultural cells (hiPSC-SNs) were fixed in 2% PFA
512 in PBS solution for 5 min; and for immunohistochemistry (IHC), the formalin-fixed, paraffin-
513 embedded tissue sections were deparaffinized, hydrated, and treated by heat-induced antigen
514 epitope retrieval in 10mM citrate buffer, pH 6.0. Non-specific binding was reduced by incubating
515 the ICC samples and IHC sections for 30 min with a solution of 5% BSA in PBS containing 0.05%
516 Tween20 (PBST). Samples were first immunolabeled with the selected primary antibodies: mouse
517 GFP (1:500, Santa Cruz Biotechnology, SCB, CA. sc9996), rabbit GFP (1:500, Cell Signaling,

Danvers, MA. 2555), rabbit $Ca_V3.2$ (1:400, Alomone, Jerusalem, Israel. ACC025), mouse Tubb3 (Tubb3, 1:500, SCB, sc-80016), IB4 (ThermoFisher LF/I21413, 1.0μg/ml), mouse CGRP (1:500, SCB, sc57053), mouse NeuN (1:100, ThermoFisher, MAB377), and rabbit GFAP (1:1000, Dako, CA. Z0334), as described previously;[13,86] in a humid atmosphere overnight at 4°C. All antibodies were diluted in PBS containing 0.05% Triton X-100 and 5% bovine serum albumin (BSA). Normal immunoglobulin G (IgG, Invitrogen) from the same species as the first antibody was replaced for the first antibody as the negative controls. The appropriate fluorophore-conjugated (Alexa 488 or Alexa 594, 1:2000) secondary antibodies (Jackson ImmunoResearch, West Grove, PA) were used to reveal immune complexes. To avoid false-positive results attributable to cross-binding in double-label combinations, each primary antibody raised in a different species was used. The immunostaining was examined, and images were captured using a Nikon TE2000-S fluorescence microscope (El Segundo, CA) with filters suitable for selectively detecting the green and red fluorescence using a QuantiFire digital camera (Optronics, Ontario, NY). For double labelling colocalization, images from the same specimen but showing different antigen signals were overlaid by digitally merging the captured images. For measurement and quantification of immunostaining, positive marker antibody immunostainings were defined as the cells with the fluorescence intensity greater than average background fluorescence plus 2 standard deviations of the cells in an adjacent area in the same ICC and IHC slide of negative control (the first antibody omitted) under identical acquisition parameters (n=10 for different markers), identified by Hoechst counterstain at a different wavelength. NIH ImageJ software (http://rsbweb.nih.gov/ij/) was used for analysis, and the brightness and contrast of the acquired fluorescence images were uniformly adjusted on ImageJ for presentation.

Quantitative PCR for AAV genome detection

Total DNA was purified from rat tissues using the DNeasy Tissue and Blood Kit (Qiagen, Valencia, CA, USA) following the manufacturer's instructions. A plasmid standard curve was generated by dilution of the plasmid AAV6.2FF-Co3.2iPA in serial tenfold dilutions in Tris-EDTA buffer (TE) and plasmid standards were mixed with 10ng/µl genomic DNA extracted from DRG of naïve rats to have AAV6.2FF-Co3.2iPA in plasmid standards ranging from $1x10^2$ copies/µl to 1×10^{18} copies/µl (**Suppl. Fig. 4**). The number of copies per standard was calculated using the online resource (https://www.technologynetworks.com/tn). Two microliters of each standard were used per qPCR reaction. The R^2 value was consistently ≥0.99. Primers corresponding to the WPRE sequence within the AAV6.2FF-CBA-Co3.2iPA vector were designed using MacVector 18.6.1 (Apex, NC). Forward: 5′-GGCTGTTGGGCACTGACAAT-3′ and reverse: 5′-CCGAAGGGACGTAGCAGAAG-3′. PCR reactions were set up with the PowerSYBR master mix (Applied Biosystems, Foster City, CA) with 2 µl of DNA (5 µl of CSF and serum) and 200 nM of each primer in a total volume of 20 µl. The primers were evaluated for amplification efficiency, the background signal from naive rat tissue, and the consistency of replicate wells using the standard thermocycling conditions for the Bio-Rad C1000 PCR system. The qPCR was performed with 1 cycle of 1 min at 95°C, followed by 40 cycles at 95 °C for 10 seconds (s) and 60 °C for 15 s. The presence of only one product was confirmed by performing a melt cycle. The assay was first developed and validated for control rat tissues, CSF, and serum (n=4). The controls used were no DNA control (nuclease-free water) and negative control (naive rat total DNA). Positive controls were DNA from DRG tissue of naïve rats, spiked with 500 copies of AAV plasmid. The no template controls were negative in each run. Two nanograms of genomic DNA from rat

563 tissues of DRG, sciatic nerve, spinal cord, brain cortex, heart, liver, kidney, and biofluids (blood
564 and CSF) were tested per PCR reaction, and samples were tested in triplicate.
565
566 **Immunoblot**
567 HEK and HiPSC-SN cell lysates from cultured cells were prepared, and immunoblots were
568 performed as described previously.[13] Cell lysates were extracted and solubilized under rotation at
569 4°C for 1 h. Insoluble proteins were removed by centrifugation at 12,000 g at 4 °C for 5 min. To
570 examine the subcellular localization of 3.2iPA1/2 and Co3.2iPA, the cells were homogenized and
571 then extracted to obtain cytosol, plasma membrane (PM), and nuclear fractions using the
572 ProteoExtract Subcellular Proteome Extraction Kit (Millipore, Billerica, MA), according to the
573 manufacturer's instructions. Protein concentration was determined using Pierce BCA kit
574 (ThermoFisher). Equivalent protein samples were size separated using 10% or 4-20% SDS-PAGE
575 gels (Bio-Rad, Hercules, CA), transferred to Immun-Blot PVDF membranes (Bio-Rad), and
576 blocked for 1 hr in 5% skim milk. The transferred PVDF membranes were subsequently incubated
577 overnight at 4°C with appropriate antibodies: mouse GFP (1:1000), mouse Na^+/K^+
578 ATPase1α (NKA1α, 1:600, SCB, sc514614), mouse Lamin B1 (1:1000, Proteintech, 66095), and
579 mouse Gapdh (1:5000, Sigma-Aldrich, SAB1403850). Immunoreactive proteins were detected by
580 Pierce enhanced chemiluminescence (ThermoFisher) on a ChemiDoc Imaging system (Bio-Rad)
581 after incubation for 1 hr with HRP-conjugated second antibodies (1:5000, Bio-Rad).
582
583 **GFP affinity pull-down followed by immunoblots, silver staining, mass spectrometry, and**
584 **PIP strip assay**

585 ***GFP affinity pull-down***. This was performed using ChromoTek GFP-Trap kit, as we described
586 previously.[26] Briefly, HEK3.2 cells were transiently transfected to express designed constructs.
587 After 48 h, cells were lysed with ice-cold nondenaturing lysis buffer containing (in mM): 10
588 Tris/Cl pH 7.5, 150 NaCl, 0.5 EDTA, with 0.5 % Nonidet P40 substitute (a non-ionic and non-
589 denaturing detergent), and protease inhibitor cocktail. The extracted cell lysates were diluted with
590 300 μL of dilution buffer containing (in mM) 10 Tris/Cl pH 7.5, 150 NaCl, 0.5 EDTA. For GFP-
591 affinity pulldown, GFP-Trap Agarose Beads were equilibrated by adding 25 μL to 1.5 μL reaction
592 tube with 500 μL of dilution buffer, cell lysates (2.5 mg total protein per sample) were incubated
593 with GFP-Trap agarose by tube rotated end-over-end overnight at 4°C, followed by precipitation
594 of beads by centrifugation at 12,000 rpm.
595 ***Silver stain, $Ca_V3.2$ immunoblot, and mass spectrometry***. The extracted cell lysates (input) and
596 GFP-affinity pulldown beads (pulldown) were performed for 4-20% SDS-PAGE gel, followed by
597 silver stain using Pierce silver stain kit (ThermoFisher) and immunoblot using $Ca_V3.2$ antibody on
598 an additional SDS-PAGE gel. The stained gel regions of interest were excised and in-gel trypsin
599 digested, as described previously.[26,87] Extracted tryptic peptides were analyzed by nLC-MS/MS
600 using a nanoACQUITY (Waters Corporation, Milford, MA) online coupled with an Orbitrap Velos
601 Pro hybrid ion trap mass spectrometer (ThermoFisher).[26] The precursor ions were selected
602 automatically by the instrument. Resultant MS/MS data were analyzed using the Mascot search
603 engine (Matrix Science version 2.4) against the SWISSPROT human database.
604 ***PIP strip assay***.[26] N2A cells transfected with GFP-Co3.2iPA and GFP-CoNP were prepared for
605 cell lysate using a denaturing RIPA buffer containing (in mM): 10 Tris-HCl pH 7.5, 150 NaCl, 0.5
606 EDTA, with 0.1% SDS, 1% Triton X100, 1% deoxycholate, and protease inhibitor cocktail. The
607 GFP-affinity pulldown beads from N2A cells were size separated using 4-20% SDS-PAGE gels

608 followed by silver stain. PIP strip assay (Echelon Biosciences, Salt Lake City, UT) was performed
609 to analyze interactions between purified GFP-Co3.2iPA from N2A cells and membrane lipids,
610 compared to purified GFP-CoNP as control. In brief, PIP (phosphatidylinositol phosphate) strip
611 membranes were blocked in 3% (w/v) fatty acid-free BSA (Sigma-Aldrich) in TBST (50 mM Tris-
612 HCl, pH 7.5, 150 mM NaCl, and 0.1% Tween 20) for 1 h. The membranes were then incubated in
613 the same solution with the purified GFP-Co3.2iPA or GFP-CoNP (equal to 1.5 mg/mL) overnight
614 at 4°C with gentle agitation. The membranes were washed 3 times over 30 min in fatty acid-free
615 BSA-TBST. The membranes were incubated for 1h with 1:2000 dilution of HRP conjugated anti-
616 GFP monoclonal antibody (Proteintech, HRP66002) at room temperature, then washed 6 times
617 over 1 h in TBST, and the protein that was bound to the membrane by interaction with
618 phospholipids was detected by enhanced chemiluminescence on a ChemiDoc Imaging system.
619 PIP2 lipid spots: LPA, Lysophosphatidic acid; LPC, Lysophosphocholine; PtdIns,
620 Phosphatidylinositol; PtdIns(3)P, Phosphatidylinositol (3) phosphate; PtdIns(4)P,
621 Phosphatidylinositol (4) phosphate; PtdIns(5)P, Phosphatidylinositol (5) phosphate; PE
622 Phosphatidylethanolamine; PC, Phosphatidylcholine; S1P, Sphingosine 1-Phosphate;
623 PtdIns(3,4)P_2, Phosphatidylinositol (3,4) bisphosphate; PtdIns(3,5)P_2, Phosphatidylinositol (3,5)
624 bisphosphate; PtdIns(4,5)P_2, Phosphatidylinositol (4,5) bisphosphate; PtdIns(3,4,5)P_3,
625 Phosphatidylinositol (3,4,5) trisphosphate; PA, Phosphatidic acid; PS, Phosphatidylserine.
626
627 **Electrophysiological (EP) recordings**
628 Whole-cell voltage and current clamp recordings were performed at room temperature (28°C) to
629 measure ion channel currents and actional potentials, respectively, with an Axopatch 700B
630 amplifier (Molecular Devices, Downingtown, PA), a Digidata 1440A digitizer data acquisition

631 system (Axon Instruments), and pClamp10 software (Molecular Devices, San Jose, CA).[13,26] The
632 composition of the pipette and external solution for recording ion channel currents on HEK3.2
633 cells and hiPSC-SNs were the same as described previously.[13,26] Experiments were performed in
634 a blind manner where the electrophysiologist was not aware of the treatment. Patch pipettes,
635 ranging from 0.9–2.5MΩ resistance, were formed from borosilicate glass (King Precision Glass
636 Co., Claremont, CA) and fire-polished. Recordings were made with an Axopatch 700B amplifier
637 (Molecular Devices, Downingtown, PA). Signals were filtered at 5 kHz and sampled at 20 kHz
638 with a Digidata 1440A digitizer and pClamp10 software (Molecular Devices, San Jose, CA).
639 Current density was obtained by dividing the maximum peak current (pA) by the cell capacitance
640 (pF). To determine the conductance-voltage (I–V) relationships of voltage-dependent activation,
641 the peak current densities during each voltage command step were fitted to a smooth curve with a
642 Boltzmann equation, as previously described.[13] Series resistance (3–5MΩ) was monitored before
643 and after the recordings. After achieving the whole-cell recording, capacitance (Cm) and series
644 resistance (Rs) were compensated accordingly. Voltage errors defined by Rs multiplied by peak
645 current (pA) were minimized by using 80% series resistance compensation. Cells were excluded
646 if the voltage error exceeded 5mV. All experiments were performed at room temperature
647 (22~25°C). To isolate TTX-R channels from the full complement of Na_V channels expressed in h-
648 iPSC-SNs, the extracellular bath solution contained 1 μM TTX, 20 mM TEA, 0.1 mM $CdCl_2$, and
649 intracellular pipette solution contained 140 mM CsF. EP recording was performed in differentiated
650 hiPSC-SNs at DIV14-28 that have extensive neurites. To isolate somatic I_{Na}, a brief prepulse to
651 voltage (-40mV) near spike inactivating h-iPSC-SN axonal spike but not somatic spikes was
652 performed, as described previously.[78,88] Whole-cell current-clamp recording of hiPSC-SNs was
653 performed, as described previously.[13,26] In brief, APs were generated by injection of a series of

current pulses (10 to 100 pA in steps of 10 pA, 300 ms). The baseline potentials were recorded for 20 ms before the stimulus pulses were injected into the iPSC-SNs. Resting membrane potential (RMP) was defined as the mean value of the 20 ms pre-stimulus potential in the first trial and the AP rheobase as the minimum current required to evoke the first AP. The iPSC-SNs with stable RMP more negative than -40 mV and overshooting APs (>80 mV RMP to peak) were used for additional data collection. AP frequency was determined by quantifying the number of APs elicited in response to depolarizing current injections (300 ms).

Statistics

Statistical analysis was performed with GraphPad PRISM 10 (GraphPad Software, San Diego, CA). For animal behavior evaluation, sensory behavioral changes compared to pre-treatment baseline (tBL) and between groups for von Frey and Heat measurements were generated using repeated measures two-way ANOVA and Tukey post hoc for within Co3.2iPA group and Bonferroni test for between groups. Pin and cold test results were performed by Friedman's tests and Dunn post hoc. In the treatment protocol of established pain, the measures immediately before AAV injection on the 14^{th} day post-TNI were used as the treatment baseline (tBL). AAV treatment data were also presented as a behavior reversal index, a derived value that defines the magnitude of treatment-induced reduction by quantifying the percentage of pain behavior of each modality compared to the tBL hypersensitization values (100%), in each test point and averaged reduction in treatment periods of 3.5 months. CPP difference scores were compared between vectors by Student’s t test. The estimated numbers of animals needed for behaviors were derived from our previous experience with similar experiments and the statistical analyses were done afterward

without interim data analysis.[13] Differences in the electrophysiological recordings were analyzed by one-way ANOVA and Tukey post hoc.

Data availability

All experimental data generated or analyzed in this study are either included in this article (and its supplementary information files) or will be made available upon reasonable request to the corresponding author. All AAV-encoded analgesic Co3.2iPA employed in this study were meticulously designed, developed, and produced in-house with exclusive intellectual property rights and are available by contacting the corresponding author.

Acknowledgments

This research was supported by grants from the NIH R33NS116203 and R21NS137014-01; 2021 (Catalyst) and 2023 (Transformational) awards from Dr. Ralph and Marian Falk Medical Research Trust, Bank of America, Private Bank; and Advancing a Healthier Wisconsin Endowment Project (5520680 and 5520739). The authors thank Dr. Kevin Boggs, Director of Technology Development, MCW, for overseeing the intellectual properties of analgesic iPAs.

Author contributions

HY conceived and designed the study. SMS and HY wrote the manuscript. HY and QHH revised the manuscript. SMS, BIZ, FF, and HY performed experiments, analyzed data, and organized all figures. HY and QH obtained funding.

Declaration of interests

The authors declare that the research was conducted without any commercial or financial relationships that could potentially create a conflict of interest.

Keywords. Molecular therapy, Chronic pain, Primary sensory neurons, Adeno-associated virus, Calcium channel 3.2 (Cav3.2), Inhibitory peptide aptamer

References

1 Dzau, V. J. & Pizzo, P. A. Relieving pain in America: insights from an Institute of Medicine committee. *JAMA* **312**, 1507-1508, doi:10.1001/jama.2014.12986 (2014).

2 Emery, E. C. & Wood, J. N. Gaining on Pain. *N Engl J Med* **379**, 485-487, doi:10.1056/NEJMcibr1803720 (2018).

3 Finnerup, N. B., Kuner, R. & Jensen, T. S. Neuropathic Pain: From Mechanisms to Treatment. *Physiol Rev* **101**, 259-301, doi:10.1152/physrev.00045.2019 (2021).

4 North, R. Y., Lazaro, T. T. & Dougherty, P. M. Ectopic Spontaneous Afferent Activity and Neuropathic Pain. *Neurosurgery* **65**, 49-54, doi:10.1093/neuros/nyy119 (2018).

5 Raja, S. N., Ringkamp, M., Guan, Y. & Campbell, J. N. John J. Bonica Award Lecture: Peripheral neuronal hyperexcitability: the "low-hanging" target for safe therapeutic strategies in neuropathic pain. *Pain* **161 Suppl 1**, S14-S26, doi:10.1097/j.pain.0000000000001838 (2020).

6 Baron, R. Mechanisms of disease: neuropathic pain--a clinical perspective. *Nat Clin Pract Neurol* **2**, 95-106, doi:10.1038/ncpneuro0113 (2006).

7 Ovsepian, S. V. & Waxman, S. G. Gene therapy for chronic pain: emerging opportunities in target-rich peripheral nociceptors. *Nat Rev Neurosci*, doi:10.1038/s41583-022-00673-7 (2023).

8 Todorovic, S. M. & Jevtovic-Todorovic, V. Regulation of T-type calcium channels in the peripheral pain pathway. *Channels (Austin)* **1**, 238-245 (2007).

9 Bourinet, E., Francois, A. & Laffray, S. T-type calcium channels in neuropathic pain. *Pain* **157 Suppl 1**, S15-S22, doi:10.1097/j.pain.0000000000000469 (2016).

10 Cai, S., Gomez, K., Moutal, A. & Khanna, R. Targeting T-type/CaV3.2 channels for chronic pain. *Transl Res*, doi:10.1016/j.trsl.2021.01.002 (2021).

11 Li, Y., Tatsui, C. E., Rhines, L. D., North, R. Y., Harrison, D. S., Cassidy, R. M. *et al.* Dorsal root ganglion neurons become hyperexcitable and increase expression of voltage-gated T-type calcium channels (Cav3.2) in paclitaxel-induced peripheral neuropathy. *Pain* **158**, 417-429, doi:10.1097/j.pain.0000000000000774 (2017).

12 Gambeta, E., Gandini, M. A., Souza, I. A. & Zamponi, G. W. CaV3.2 calcium channels contribute to trigeminal neuralgia. *Pain*, doi:10.1097/j.pain.0000000000002651 (2022).

13 Shin, S. M., Lauzadis, J., Itson-Zoske, B., Cai, Y., Fan, F., Natarajan, G. K. *et al.* Targeting intrinsically disordered regions facilitates discovery of calcium channels 3.2 inhibitory peptides for adeno-associated virus-mediated peripheral analgesia. *Pain* **163**, 2466-2484, doi:10.1097/j.pain.0000000000002650 (2022).

14 Itson-Zoske, B., Shin, S. M., Xu, H., Qiu, C., Fan, F., Hogan, Q. H. *et al.* Selective block of sensory neuronal T-type/Cav3.2 activity mitigates neuropathic pain behavior in a rat model of osteoarthritis pain. *Arthritis Res Ther* **24**, 168, doi:10.1186/s13075-022-02856-0 (2022).

15 Shiers, S., Klein, R. M. & Price, T. J. Quantitative differences in neuronal subpopulations between mouse and human dorsal root ganglia demonstrated with RNAscope in situ hybridization. *Pain* **161**, 2410-2424, doi:10.1097/j.pain.0000000000001973 (2020).

16 Jung, M., Dourado, M., Maksymetz, J., Jacobson, A., Laufer, B. I., Baca, M. *et al.* Cross-species transcriptomic atlas of dorsal root ganglia reveals species-specific programs for sensory function. *Nat Commun* **14**, 366, doi:10.1038/s41467-023-36014-0 (2023).

17 Xiong, C., Chua, K. C., Stage, T. B., Priotti, J., Kim, J., Altman-Merino, A. *et al.* Human Induced Pluripotent Stem Cell Derived Sensory Neurons are Sensitive to the Neurotoxic Effects of Paclitaxel. *Clin Transl Sci* **14**, 568-581, doi:10.1111/cts.12912 (2021).

18 Guimaraes, M. Z. P., De Vecchi, R., Vitoria, G., Sochacki, J. K., Paulsen, B. S., Lima, I. *et al.* Generation of iPSC-Derived Human Peripheral Sensory Neurons Releasing Substance P Elicited by TRPV1 Agonists. *Front Mol Neurosci* **11**, 277, doi:10.3389/fnmol.2018.00277 (2018).

19 Lindhout, F. W., Kooistra, R., Portegies, S., Herstel, L. J., Stucchi, R., Snoek, B. L. *et al.* Quantitative mapping of transcriptome and proteome dynamics during polarization of human iPSC-derived neurons. *Elife* **9**, doi:10.7554/eLife.58124 (2020).

20 Deng, T., Jovanovic, V. M., Tristan, C. A., Weber, C., Chu, P. H., Inman, J. *et al.* Scalable generation of sensory neurons from human pluripotent stem cells. *Stem Cell Reports* **18**, 1030-1047, doi:10.1016/j.stemcr.2023.03.006 (2023).

21 Li, R., Walsh, P., Truong, V., Petersen, A., Dutton, J. R. & Hubel, A. Differentiation of Human iPS Cells Into Sensory Neurons Exhibits Developmental Stage-Specific Cryopreservation Challenges. *Front Cell Dev Biol* **9**, 796960, doi:10.3389/fcell.2021.796960 (2021).

22 Chen, X., Zaro, J. L. & Shen, W. C. Fusion protein linkers: property, design and functionality. *Adv Drug Deliv Rev* **65**, 1357-1369, doi:10.1016/j.addr.2012.09.039 (2013).

23 van Lieshout, L. P., Domm, J. M., Rindler, T. N., Frost, K. L., Sorensen, D. L., Medina, S. J. *et al.* A Novel Triple-Mutant AAV6 Capsid Induces Rapid and Potent Transgene Expression in the Muscle and Respiratory Tract of Mice. *Mol Ther Methods Clin Dev* **9**, 323-329, doi:10.1016/j.omtm.2018.04.005 (2018).

24 Mogil, J. S. Sex differences in pain and pain inhibition: multiple explanations of a controversial phenomenon. *Nat Rev Neurosci* **13**, 859-866, doi:10.1038/nrn3360 (2012).

25 Shin, S. M., Itson-Zoske, B., Fan, F., Gani, U., Rahman, M., Hogan, Q. H. *et al.* Peripheral sensory neurons and non-neuronal cells express functional Piezo1 channels. *Mol Pain* **19**, 17448069231174315, doi:10.1177/17448069231174315 (2023).

26 Shin, S. M., Itson-Zoske, B., Fan, F., Xiao, Y., Qiu, C., Cummins, T. R. *et al.* Peripherally targeted analgesia via AAV-mediated sensory neuron-specific inhibition of multiple pronociceptive sodium channels. *J Clin Invest*, doi:10.1172/JCI170813 (2024).

27 Farrar, J. T., Berlin, J. A. & Strom, B. L. Clinically important changes in acute pain outcome measures: a validation study. *J Pain Symptom Manage* **25**, 406-411, doi:10.1016/s0885-3924(03)00162-3 (2003).

28 McQuay, H. J., Barden, J. & Moore, R. A. Clinically important changes-what's important and whose change is it anyway? *J Pain Symptom Manage* **25**, 395-396, doi:10.1016/s0885-3924(03)00099-x (2003).

29 McDonnell, A., Collins, S., Ali, Z., Iavarone, L., Surujbally, R., Kirby, S. *et al.* Efficacy of the Nav1.7 blocker PF-05089771 in a randomised, placebo-controlled, double-blind clinical study in subjects with painful diabetic peripheral neuropathy. *Pain* **159**, 1465-1476, doi:10.1097/j.pain.0000000000001227 (2018).

30 Dworkin, R. H., Evans, S. R., Mbowe, O. & McDermott, M. P. Essential statistical principles of clinical trials of pain treatments. *Pain Rep* **6**, e863, doi:10.1097/PR9.0000000000000863 (2021).

797 31 Yu, H., Shin, S. M., Xiang, H., Chao, D., Cai, Y., Xu, H. *et al.* AAV-encoded CaV2.2 peptide
798 aptamer CBD3A6K for primary sensory neuron-targeted treatment of established
799 neuropathic pain. *Gene Ther* **26**, 308-323, doi:10.1038/s41434-019-0082-7 (2019).
800 32 Park, C., Park, D., Hassan, Z. U., Choi, S. H. & Kim, S. Comparison of RT-qPCR and RT-
801 ddPCR with Rift valley fever virus (RVFV) RNA. *Sci Rep* **13**, 3085, doi:10.1038/s41598-
802 023-29023-y (2023).
803 33 Hendus-Altenburger, R., Vogensen, J., Pedersen, E. S., Luchini, A., Araya-Secchi, R.,
804 Bendsoe, A. H. *et al.* The intracellular lipid-binding domain of human Na(+)/H(+) exchanger
805 1 forms a lipid-protein co-structure essential for activity. *Commun Biol* **3**, 731,
806 doi:10.1038/s42003-020-01455-6 (2020).
807 34 Wang, Z. Z., Shi, X. X., Huang, G. Y., Hao, G. F. & Yang, G. F. Fragment-based drug design
808 facilitates selective kinase inhibitor discovery. *Trends Pharmacol Sci* **42**, 551-565,
809 doi:10.1016/j.tips.2021.04.001 (2021).
810 35 Arbesu, M., Iruela, G., Fuentes, H., Teixeira, J. M. C. & Pons, M. Intramolecular Fuzzy
811 Interactions Involving Intrinsically Disordered Domains. *Front Mol Biosci* **5**, 39,
812 doi:10.3389/fmolb.2018.00039 (2018).
813 36 Hille, B., Dickson, E. J., Kruse, M., Vivas, O. & Suh, B. C. Phosphoinositides regulate ion
814 channels. *Biochim Biophys Acta* **1851**, 844-856, doi:10.1016/j.bbalip.2014.09.010 (2015).
815 37 Deryusheva, E., Nemashkalova, E., Galloux, M., Richard, C. A., Eleouet, J. F., Kovacs, D. *et*
816 *al.* Does Intrinsic Disorder in Proteins Favor Their Interaction with Lipids? *Proteomics* **19**,
817 e1800098, doi:10.1002/pmic.201800098 (2019).
818 38 Kaur, G., Pinggera, A., Ortner, N. J., Lieb, A., Sinnegger-Brauns, M. J., Yarov-Yarovoy, V. *et*
819 *al.* A Polybasic Plasma Membrane Binding Motif in the I-II Linker Stabilizes Voltage-gated

CaV1.2 Calcium Channel Function. *J Biol Chem* **290**, 21086-21100, doi:10.1074/jbc.M115.645671 (2015).

39 Temmerman, K., Ebert, A. D., Muller, H. M., Sinning, I., Tews, I. & Nickel, W. A direct role for phosphatidylinositol-4,5-bisphosphate in unconventional secretion of fibroblast growth factor 2. *Traffic* **9**, 1204-1217, doi:10.1111/j.1600-0854.2008.00749.x (2008).

40 Yamasaki, K., Daiho, T., Yasuda, S., Danko, S., Kawabe, J. I. & Suzuki, H. Electrostatic interactions between single arginine and phospholipids modulate physiological properties of sarcoplasmic reticulum Ca(2+)-ATPase. *Sci Rep* **12**, 12200, doi:10.1038/s41598-022-16091-9 (2022).

41 Zeng, X., Ruff, K. M. & Pappu, R. V. Competing interactions give rise to two-state behavior and switch-like transitions in charge-rich intrinsically disordered proteins. *Proc Natl Acad Sci U S A* **119**, e2200559119, doi:10.1073/pnas.2200559119 (2022).

42 Jacus, M. O., Uebele, V. N., Renger, J. J. & Todorovic, S. M. Presynaptic Cav3.2 channels regulate excitatory neurotransmission in nociceptive dorsal horn neurons. *J Neurosci* **32**, 9374-9382, doi:10.1523/JNEUROSCI.0068-12.2012 (2012).

43 Zhang, L., Li, S. & Xia, M. High-Throughput Neurite Outgrowth Assay Using GFP-Labeled iPSC-Derived Neurons. *Curr Protoc* **2**, e542, doi:10.1002/cpz1.542 (2022).

44 Aguado, C., Garcia-Madrona, S., Gil-Minguez, M. & Lujan, R. Ontogenic Changes and Differential Localization of T-type Ca(2+) Channel Subunits Cav3.1 and Cav3.2 in Mouse Hippocampus and Cerebellum. *Front Neuroanat* **10**, 83, doi:10.3389/fnana.2016.00083 (2016).

45 Molineux, M. L., McRory, J. E., McKay, B. E., Hamid, J., Mehaffey, W. H., Rehak, R. *et al.* Specific T-type calcium channel isoforms are associated with distinct burst phenotypes in

deep cerebellar nuclear neurons. *Proc Natl Acad Sci U S A* **103**, 5555-5560, doi:10.1073/pnas.0601261103 (2006).

46 Clarke, R. J. Electrostatic switch mechanisms of membrane protein trafficking and regulation. *Biophys Rev* **15**, 1967-1985, doi:10.1007/s12551-023-01166-2 (2023).

47 Demers-Giroux, P. O., Bourdin, B., Sauve, R. & Parent, L. Cooperative activation of the T-type CaV3.2 channel: interaction between Domains II and III. *J Biol Chem* **288**, 29281-29293, doi:10.1074/jbc.M113.500975 (2013).

48 Monteil, A., Chausson, P., Boutourlinsky, K., Mezghrani, A., Huc-Brandt, S., Blesneac, I. *et al.* Inhibition of Cav3.2 T-type Calcium Channels by Its Intracellular I-II Loop. *J Biol Chem* **290**, 16168-16176, doi:10.1074/jbc.M114.634261 (2015).

49 Verdera, H. C., Kuranda, K. & Mingozzi, F. AAV Vector Immunogenicity in Humans: A Long Journey to Successful Gene Transfer. *Mol Ther* **28**, 723-746, doi:10.1016/j.ymthe.2019.12.010 (2020).

50 Shen, W., Liu, S. & Ou, L. rAAV immunogenicity, toxicity, and durability in 255 clinical trials: A meta-analysis. *Front Immunol* **13**, 1001263, doi:10.3389/fimmu.2022.1001263 (2022).

51 Rapti, K., Louis-Jeune, V., Kohlbrenner, E., Ishikawa, K., Ladage, D., Zolotukhin, S. *et al.* Neutralizing antibodies against AAV serotypes 1, 2, 6, and 9 in sera of commonly used animal models. *Mol Ther* **20**, 73-83, doi:10.1038/mt.2011.177 (2012).

52 Kang, M. H., van Lieshout, L. P., Xu, L., Domm, J. M., Vadivel, A., Renesme, L. *et al.* A lung tropic AAV vector improves survival in a mouse model of surfactant B deficiency. *Nat Commun* **11**, 3929, doi:10.1038/s41467-020-17577-8 (2020).

53 Brommel, C. M., Cooney, A. L. & Sinn, P. L. Adeno-Associated Virus-Based Gene Therapy for Lifelong Correction of Genetic Disease. *Hum Gene Ther* **31**, 985-995, doi:10.1089/hum.2020.138 (2020).

54 Moreno, A. M., Aleman, F., Catroli, G. F., Hunt, M., Hu, M., Dailamy, A. *et al.* Long-lasting analgesia via targeted in situ repression of NaV1.7 in mice. *Sci Transl Med* **13**, doi:10.1126/scitranslmed.aay9056 (2021).

55 Mingozzi, F., Meulenberg, J. J., Hui, D. J., Basner-Tschakarjan, E., Hasbrouck, N. C., Edmonson, S. A. *et al.* AAV-1-mediated gene transfer to skeletal muscle in humans results in dose-dependent activation of capsid-specific T cells. *Blood* **114**, 2077-2086, doi:10.1182/blood-2008-07-167510 (2009).

56 Waxman, S. G. & Zamponi, G. W. Regulating excitability of peripheral afferents: emerging ion channel targets. *Nat Neurosci* **17**, 153-163, doi:10.1038/nn.3602 (2014).

57 Pfirrmann, C. W., Oberholzer, P. A., Zanetti, M., Boos, N., Trudell, D. J., Resnick, D. *et al.* Selective nerve root blocks for the treatment of sciatica: evaluation of injection site and effectiveness--a study with patients and cadavers. *Radiology* **221**, 704-711, doi:10.1148/radiol.2213001635 (2001).

58 Fischer, G., Kostic, S., Nakai, H., Park, F., Sapunar, D., Yu, H. *et al.* Direct injection into the dorsal root ganglion: technical, behavioral, and histological observations. *J Neurosci Methods* **199**, 43-55, doi:10.1016/j.jneumeth.2011.04.021 (2011).

59 Hoffmann, T., Sharon, O., Wittmann, J., Carr, R. W., Vyshnevska, A., Col, R. *et al.* NaV1.7 and pain: contribution of peripheral nerves. *Pain* **159**, 496-506, doi:10.1097/j.pain.0000000000001119 (2018).

60 Ovsepian, S. V. & Waxman, S. G. Gene therapy for chronic pain: emerging opportunities in target-rich peripheral nociceptors. *Nat Rev Neurosci* **24**, 252-265, doi:10.1038/s41583-022-00673-7 (2023).

61 Xu, J., Sun, Z., Wu, J., Rana, M., Garza, J., Zhu, A. C. *et al.* Peripheral Nerve Stimulation in Pain Management: A Systematic Review. *Pain Physician* **24**, E131-E152 (2021).

62 Shin, S. M., Wang, F., Qiu, C., Itson-Zoske, B., Hogan, Q. H. & Yu, H. Sigma-1 receptor activity in primary sensory neurons is a critical driver of neuropathic pain. *Gene Ther*, doi:10.1038/s41434-020-0157-5 (2020).

63 Hordeaux, J., Buza, E. L., Dyer, C., Goode, T., Mitchell, T. W., Richman, L. *et al.* Adeno-Associated Virus-Induced Dorsal Root Ganglion Pathology. *Hum Gene Ther* **31**, 808-818, doi:10.1089/hum.2020.167 (2020).

64 Buss, N., Lanigan, L., Zeller, J., Cissell, D., Metea, M., Adams, E. *et al.* Characterization of AAV-mediated dorsal root ganglionopathy. *Mol Ther Methods Clin Dev* **24**, 342-354, doi:10.1016/j.omtm.2022.01.013 (2022).

65 Johnson, E. W., Sutherland, J. J., Meseck, E., McElroy, C., Chand, D. H., Tukov, F. F. *et al.* Neurofilament light chain and dorsal root ganglia injury after adeno-associated virus 9 gene therapy in nonhuman primates. *Mol Ther Methods Clin Dev* **28**, 208-219, doi:10.1016/j.omtm.2022.12.012 (2023).

66 Beutler, A. S. & Reinhardt, M. AAV for pain: steps towards clinical translation. *Gene Ther* **16**, 461-469, doi:10.1038/gt.2009.23 (2009).

67 Pleticha, J., Maus, T. P. & Beutler, A. S. Future Directions in Pain Management: Integrating Anatomically Selective Delivery Techniques With Novel Molecularly Selective Agents. *Mayo Clin Proc* **91**, 522-533, doi:10.1016/j.mayocp.2016.02.015 (2016).

68 Pleticha, J., Maus, T. P., Christner, J. A., Marsh, M. P., Lee, K. H., Hooten, W. M. *et al.* Minimally invasive convection-enhanced delivery of biologics into dorsal root ganglia: validation in the pig model and prospective modeling in humans. Technical note. *J Neurosurg* **121**, 851-858, doi:10.3171/2014.6.JNS132364 (2014).

69 Grant, P. E., Caneris, O. A., Gonzalez, R. G., Iadarola, M. J., Sapio, M. R., Mannes, A. J. *et al.* Analgesia after dorsal root ganglionic injection under CT-guidance in a patient with intractable phantom limb pain. *Pain Med* **24**, 1122-1123, doi:10.1093/pm/pnad039 (2023).

70 Amir, R. & Devor, M. Chemically mediated cross-excitation in rat dorsal root ganglia. *J Neurosci* **16**, 4733-4741, doi:10.1523/JNEUROSCI.16-15-04733.1996 (1996).

71 Zheng, Q., Xie, W., Luckemeyer, D. D., Lay, M., Wang, X. W., Dong, X. *et al.* Synchronized cluster firing, a distinct form of sensory neuron activation, drives spontaneous pain. *Neuron* **110**, 209-220 e206, doi:10.1016/j.neuron.2021.10.019 (2022).

72 Kim, Y. S., Anderson, M., Park, K., Zheng, Q., Agarwal, A., Gong, C. *et al.* Coupled Activation of Primary Sensory Neurons Contributes to Chronic Pain. *Neuron* **91**, 1085-1096, doi:10.1016/j.neuron.2016.07.044 (2016).

73 Choi, S., Yu, E., Hwang, E. & Llinas, R. R. Pathophysiological implication of CaV3.1 T-type Ca2+ channels in trigeminal neuropathic pain. *Proc Natl Acad Sci U S A* **113**, 2270-2275, doi:10.1073/pnas.1600418113 (2016).

74 Na, H. S., Choi, S., Kim, J., Park, J. & Shin, H. S. Attenuated neuropathic pain in Cav3.1 null mice. *Mol Cells* **25**, 242-246 (2008).

75 Dib-Hajj, S. D. Human pain in a dish: Native DRG neurons and differentiated pluripotent stem cells. *Pain* **155**, 1681-1682, doi:10.1016/j.pain.2014.07.010 (2014).

76 Zurek, N. A., Ehsanian, R., Goins, A. E., Adams, I. M., Petersen, T., Goyal, S. *et al.* Electrophysiological analyses of human dorsal root ganglia and human induced pluripotent stem cell-derived sensory neurons from male and female donors. *bioRxiv*, doi:10.1101/2023.11.03.565343 (2023).

77 Walsh, P., Truong, V., Nayak, S., Saldias Montivero, M., Low, W. C., Parr, A. M. *et al.* Accelerated differentiation of human pluripotent stem cells into neural lineages via an early intermediate ectoderm population. *Stem Cells* **38**, 1400-1408, doi:10.1002/stem.3260 (2020).

78 Shin, S. M., Itson-Zoske, B., Fan, F., Xiao, Y., Qiu, C., Cummins, T. R. *et al.* Peripherally targeted analgesia via AAV-mediated sensory neuron-specific inhibition of multiple pronociceptive sodium channels. *J Clin Invest* **134**, doi:10.1172/JCI170813 (2024).

79 Yu, H., Fischer, G., Ferhatovic, L., Fan, F., Light, A. R., Weihrauch, D. *et al.* Intraganglionic AAV6 results in efficient and long-term gene transfer to peripheral sensory nervous system in adult rats. *PLoS One* **8**, e61266, doi:10.1371/journal.pone.0061266 (2013).

80 Yu, H., Fischer, G., Jia, G., Reiser, J., Park, F. & Hogan, Q. H. Lentiviral gene transfer into the dorsal root ganglion of adult rats. *Mol Pain* **7**, 63, doi:10.1186/1744-8069-7-63 (2011).

81 Xiang, H., Liu, Z., Wang, F., Xu, H., Roberts, C., Fischer, G. *et al.* Primary sensory neuron-specific interference of TRPV1 signaling by AAV-encoded TRPV1 peptide aptamer attenuates neuropathic pain. *Mol Pain* **13**, 1744806917717040, doi:10.1177/1744806917717040 (2017).

82 Griggs, R. B., Bardo, M. T. & Taylor, B. K. Gabapentin alleviates affective pain after traumatic nerve injury. *Neuroreport* **26**, 522-527, doi:10.1097/WNR.0000000000000382 (2015).

83 Park, H. J., Sandor, K., McQueen, J., Woller, S. A., Svensson, C. I., Corr, M. *et al.* The effect of gabapentin and ketorolac on allodynia and conditioned place preference in antibody-induced inflammation. *Eur J Pain* **20**, 917-925, doi:10.1002/ejp.816 (2016).

84 Juarez-Salinas, D. L., Braz, J. M., Etlin, A., Gee, S., Sohal, V. & Basbaum, A. I. GABAergic cell transplants in the anterior cingulate cortex reduce neuropathic pain aversiveness. *Brain* **142**, 2655-2669, doi:10.1093/brain/awz203 (2019).

85 Fischer, G., Wang, F., Xiang, H., Bai, X., Yu, H. & Hogan, Q. H. Inhibition of neuropathic hyperalgesia by intrathecal bone marrow stromal cells is associated with alteration of multiple soluble factors in cerebrospinal fluid. *Exp Brain Res* **235**, 2627-2638, doi:10.1007/s00221-017-5000-x (2017).

86 Yu, H., Shin, S. M., Xiang, H., Chao, D., Cai, Y., Xu, H. *et al.* AAV-encoded CaV2.2 peptide aptamer CBD3A6K for primary sensory neuron-targeted treatment of established neuropathic pain. *Gene Ther*, doi:10.1038/s41434-019-0082-7 (2019).

87 Yu, H., Wakim, B., Li, M., Halligan, B., Tint, G. S. & Patel, S. B. Quantifying raft proteins in neonatal mouse brain by 'tube-gel' protein digestion label-free shotgun proteomics. *Proteome Sci* **5**, 17, doi:10.1186/1477-5956-5-17 (2007).

88 Milescu, L. S., Bean, B. P. & Smith, J. C. Isolation of somatic Na+ currents by selective inactivation of axonal channels with a voltage prepulse. *J Neurosci* **30**, 7740-7748, doi:10.1523/JNEUROSCI.6136-09.2010 (2010).

Legend

Figure 1. Design Co3.2iPA and functional test. (A, B) Alignment of human and rat 3.2iPA1 and iPA2. (**C**) Translation of GFP fused Co3.2iPA. (**D**) Construct of AAV-encoded human Co3.2iPA and CoNP, showing the transgene cassette on the top of AAV map. (**E**) Whole-cell voltage clamp on naïve HEK3.2 cells, and 3 days after transfection of CoNP and Co3.2iPA, respectively. (**F**) I/V curve and (**G**) Peak $I_{Ca3.2}$ density analysis, ***p<0.001, one-way ANOVA and Tukey post hoc.

Figure 2. Treatment of established TNI pain by DRG delivery of AAV6.2FF-Co3.2iPA (male rats). (**A**, **B)** Silver stain of purified AAVs (**A**) used for the experiments in an animal protocol schematically outlined (**B**). (**C**-**F**) The time courses and (**C1-F1**) % of pain reduction of vF, Pin, Heat, and Cold before and after DRG injection of either AAV6.2FF-Co3.2iPA (n=9) or AAV6.2FF-NP (control, n=9). *p<0.05, **p<0.0,1 and ***p<0.001 for comparisons to the tBL within Co3.2iPA group and #p<0.05, ##p<0.01, and ###p<0.001 between CoNP and Co3.2iPA groups. Repeated measures two-way ANOVA for vF and Heat, and Tukey (within Co3.2iPA group) and Bonferroni (between CoNP and Co3.2iPA groups) post hoc; and non-parametric Friedman ANOVA for Pin and Cold tests and Dunn's post hoc. Dashed lines in panels **C1-F1** denote the absence of hypersensitivity. (**G**) Average pain relief in 3.5 months treatment course showed 52%, 49%, 69%, and 67% reduction of vF-, Pin-, Cold-, and Heat-stimulated mechanical and thermal pain behaviors, respectively. ** p<0.01 *** p<0.001, unpaired, two-tailed student's t-test. (**H**) Results of CPP scores (seconds, s) of pre-conditioning chamber and of the GBP-paired chamber in AAV6.2FF-CoNP and AAV6.2FF-Co3.2iPA animals, **p<0.001 (unpaired, two-tailed Student's t-test).

998

999 **Figure 3. IHC of GFP-NaViPA1 and target gene expression. (A)** GFP-Co3.2iPA expression in
1000 DRG 3.5 months after injection. (**B-G**) Representative double immunostaining IHC montage
1001 images of DRG sections in TNI rats illustrate colocalization of GFPCo3.2iPA with Tubb3, Cav3.2,
1002 IB4, CGRP, NKA1α, and NeuN, respectively, in PSNs. Note: multiple PSN cellular localization
1003 GFPCo3.2iPA in the cytosol, nucleus, and PM. (**H** and **I**) GFPCo3.2iPA signal was not
1004 colocalized with GFAP. Scale bar (μm): 200 for A, 100 for B-H, and 25 for I.

1005

1006 **Figure 4. QPCR of AAV6.2FF-Co3.2iPA genome.** QPCR quantification of AAV6.2FF-
1007 Co3.2iPA genome copy numbers and anatomical biodistribution 3.5 months post AAV6.2FF-
1008 Co3.2iPA injection into the right (R) L4/L5 DRG (n=6 rats). LL4/5, Left DRG; lumbar SC,
1009 lumbar spinal cord; CSF, cerebrospinal fluid.

1010

1011 **Figure 5. Analgesia of DRG-AAV6.2FF- Co3.2iPA treatment in female TNI rats.** (**A-D**)
1012 Analogous figures to Fig. 2 show significant analgesia and (**A1-D1**) % of pain reduction after DRG
1013 delivery of AAV6.2FF- Co3.2iPA in the established TNI pain behaviors of female rats. *, **, and
1014 *** denote $p<0.05$, 0.01, and 0.001 for comparisons to the treatment baseline (tBL) within the
1015 Co3.2iPA group and #$p<0.05$, ##$p<0.01$, and ###$p<0.001$ for comparisons between CoNP and
1016 Co3.2iPA groups. Repeated measures parametric two-way ANOVA for vF and Heat followed by
1017 Tukey (within Co3.2iPA group) and Bonferroni (between groups) post-hoc; and non-parametric
1018 Friedman ANOVA for Pin and Cold tests and Dunn's post hoc. Dashed lines in panels **A1-D1**
1019 denote the absence of hypersensitivity. (**E**) Average pain relief of each modality in 3.5-month
1020 treatment, ** $p<0.01$ and *** $p<0.001$ comparisons between groups (unpaired, two-tailed

Student's t-test). (**F**) CPP difference scores (s) of pre-conditioning chamber and of the GBP-paired 56chamber between AAV6.2FF-Co3.2iPA (n=9) and AAV6.2FF-CoNP (control, n=9), **p<0.01 (unpaired, two-tailed Student's t test). (**G**) Representative montage IHC images colocalization of GFP-Co3.2iPA with Tubb3, Scale bar:100μm.

Figure 6. 3.2iPA-Ca$_V$3.2 interaction and 3.2iPA binding to phospholipids. (**A**) Immunoblots of 3.2iPA1 and 3.2iPA2 (GFP fusion) in the extracted cytosol, membrane, and nuclei samples after transfection into HEK cells. Cytosol, membrane, and nuclear loading were indicated by GAPDH, NKA1a, and LamB1, respectively. (**B**, **C**) Silver-stained gel (**B**) and Ca$_V$3.2 immunoblot (**C**) of GFP-affinity pull-down beads from HEK3.2 cells transfected with GFP, GFPNP, 3.2iPA1, and 3.2iPA2. (**D**) Excised stained gel pieces ranging from 180-300 kDa (**B**, squares) from GFP+GFPNP and GFP3.2iPA1/2 samples for mass spectrometry. Representative nLC-MS/MS spectra of ions (red) matching unique Ca$_V$3.2 peptide with abundance ratio of 3.2iPA1/2 over control=100. (**E**) Silver stain on 1D SDS-PAGE gel of GFP-affinity pulldown beads in N2A cells transfected with GFP-Co3.2iPA and GFP-CoNP and cell lysates prepared using denaturing RIPA buffer and (**F**) the results of PIP strip analysis.

Figure 7. Inhibition of T-channels by Co3.2iPA in hiPSC-SNs. LV-medicated expression of NP (**A-A2**) and Co3.2iPA (**B-B2**) at MOI=5 with squares of **A2** and **B2** amplified showing in **A3** and **B3**; scale bar: 25mm. (**C**) Representative immunoblots of endogenous Ca$_V$3.2, as well as LV-transduced NP and Co3.2iPA in extracted cytosol, membrane, and nuclear samples of hiPSC-SNs. Cytosol, membrane, and nuclei loading were indicated by GAPDH, NKA1α, and LamB1, respectively. (**D-F)** EP recording traces of T-currents in naive and in the presence of CoNP and

Co3.2iPA in hiPSC-SNs (inserts: scales and pulse protocol), (**G**) I/V curves, and (**G1**) peak I_{LVA} densities; ***p<0.001, one-way ANOVA and Tukey post-hoc. (**H**, **I**) Representative AP traces elicited by 300 ms depolarizing current of 50 pA (**H**) and 100 pA (**I**) (same cells) from RMP were recorded from hiPSC-SNs, as indicated. (**J**) Comparison of responses (number of APs) in different groups across a range of step current injections from 0 to 100 pA; ***p < 0.001, two-way ANOVA of main effects of groups with Bonferroni post hoc. (**K**) Scatter plots with bars show analysis of the rheobases and (**L**) AP numbers evoked by input current at 50 pA and (**M**)100 pA, respectively. The number in each group is the number of analyzed cells per group. ***denotes <0.001, One-way ANOVA followed by Tukey post hoc.

Table 1. Abundant human Cav3.2 peptides (red) detected in GFP3.2iPA1/2 pull-down samples

Annotated Sequence	Protein O95180 position*	Ratio of 3.2iPAs /control#	MS/MS spectra of ions (control)	MS/MS spectra of ions (3.2iPAs)	Xcorr
[R].LATGLGTMNYPTILPSGVGSGK.[G]	aa 604-625	100	Not found	High	2.27
[K].VDPSAVQGQGPGHR.[Q]	aa 490-503	31.34	Peak Found	High	2
[R].VDADRPPLPQESPGAR.[D]	aa 1894-1909	100	Not found	High	2.27
[R].DGQVVALPSDFF.[I]	aa 1218-1231	100	Not found	High	2.31
[K].VLEPYKPQWCR.[S]	aa 1257-1267	8.58	Peak Found	High	3.01
[R].VPLGAPPPGPAALVGASPESPGAPGR.[E]	aa 13-38	8.13	Peak Found	High	6.17
[R].SSPCAPWGPSGAWSSR.[R]	aa 1126-1141	22.99	Peak Found	High	2.57
[R].EDAAELDDDSEDSCCLR.[L]	aa 1237-1253	100	Not found	High	3.26
[R].DSLEPTEGSGAGGDPAAK.[G]	aa 2230-2247	40.44	Peak Found	High	3.87
[R].QHQEAEEAR.[R]	aa 1563-1571	63.6	Peak Found	High	3.24
[R].GVYEFTQDVR.[H]	aa 726-735	8.21	Peak Found	High	2.43
[R].DTLDPAEPGEK.[T]	aa 2033-2043	16.89	Peak Found	High	2.19
[R].PSAAEGGSTTLR.[R]	aa 2206-2217	100	Not found	High	2.15
[R].LYSVDAQGFLDK.[P]	aa 2135-2146	100	Not found	High	1.61

Unique hCaV3.2 peptides are shown in bold italics in the table.

* O95180, human Cav3.2 protein; aa, amino acid. # Ion abundance ratio of 3.2iPAs/control (GFP and NP).

Click here to access/download;Figure (high resolution without caption);Figure 1.pdf

Figure 1

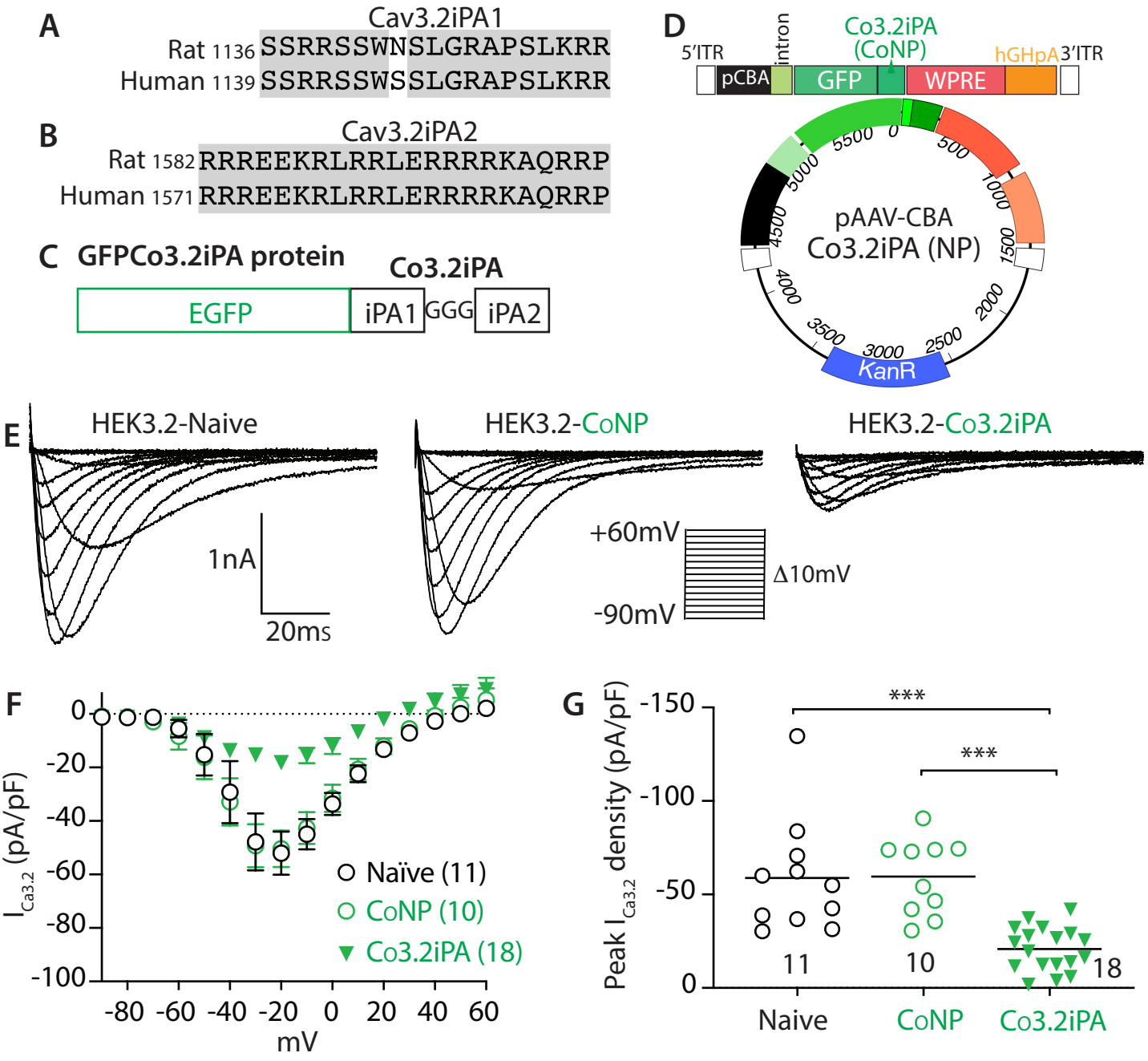

Click here to access/download;Figure (high resolution without caption);Figure 2.pdf

Figure 2

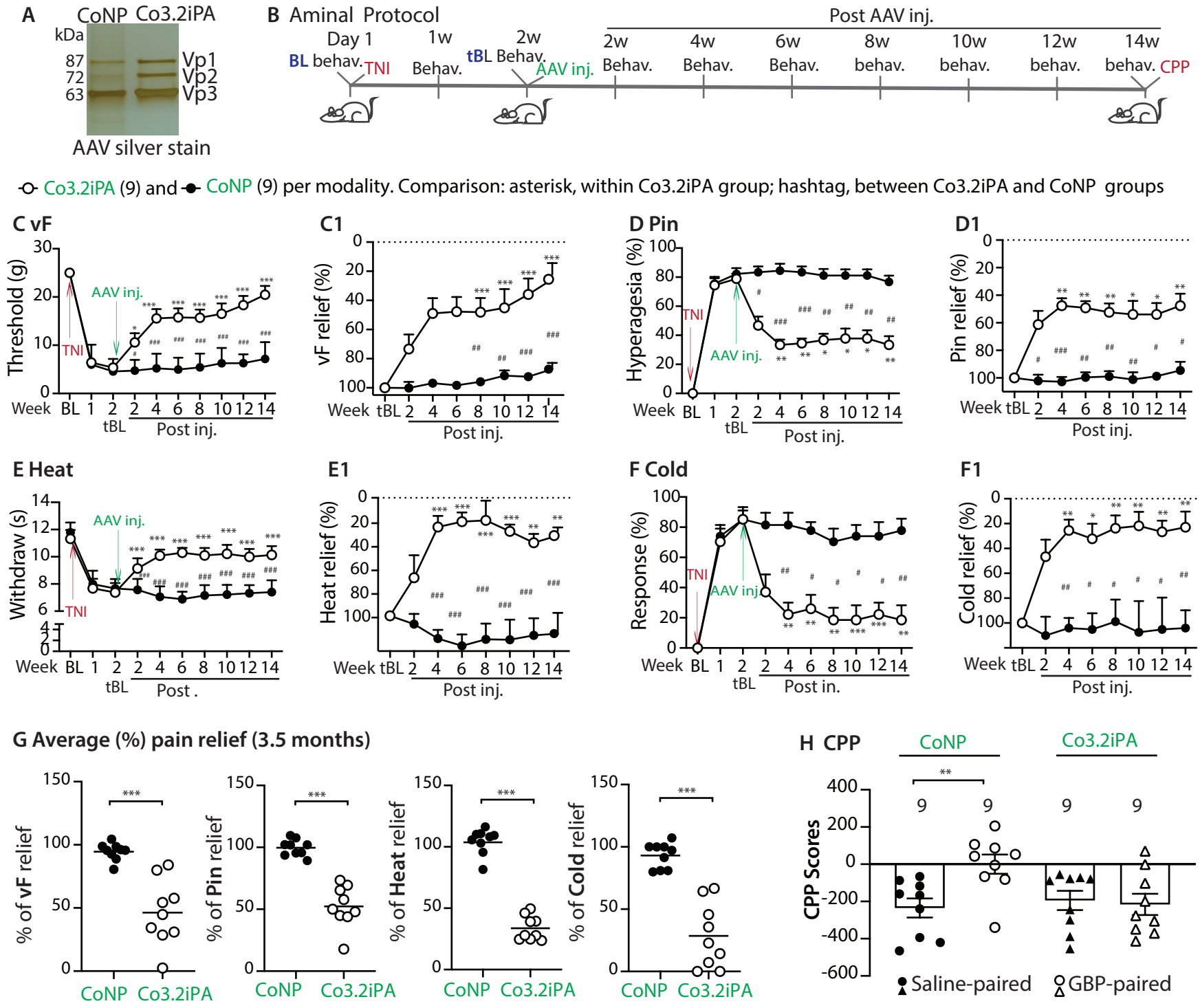

Figure 2

Figure 3

Click here to access/download;Figure (high resolution without caption);Figure 3.pdf

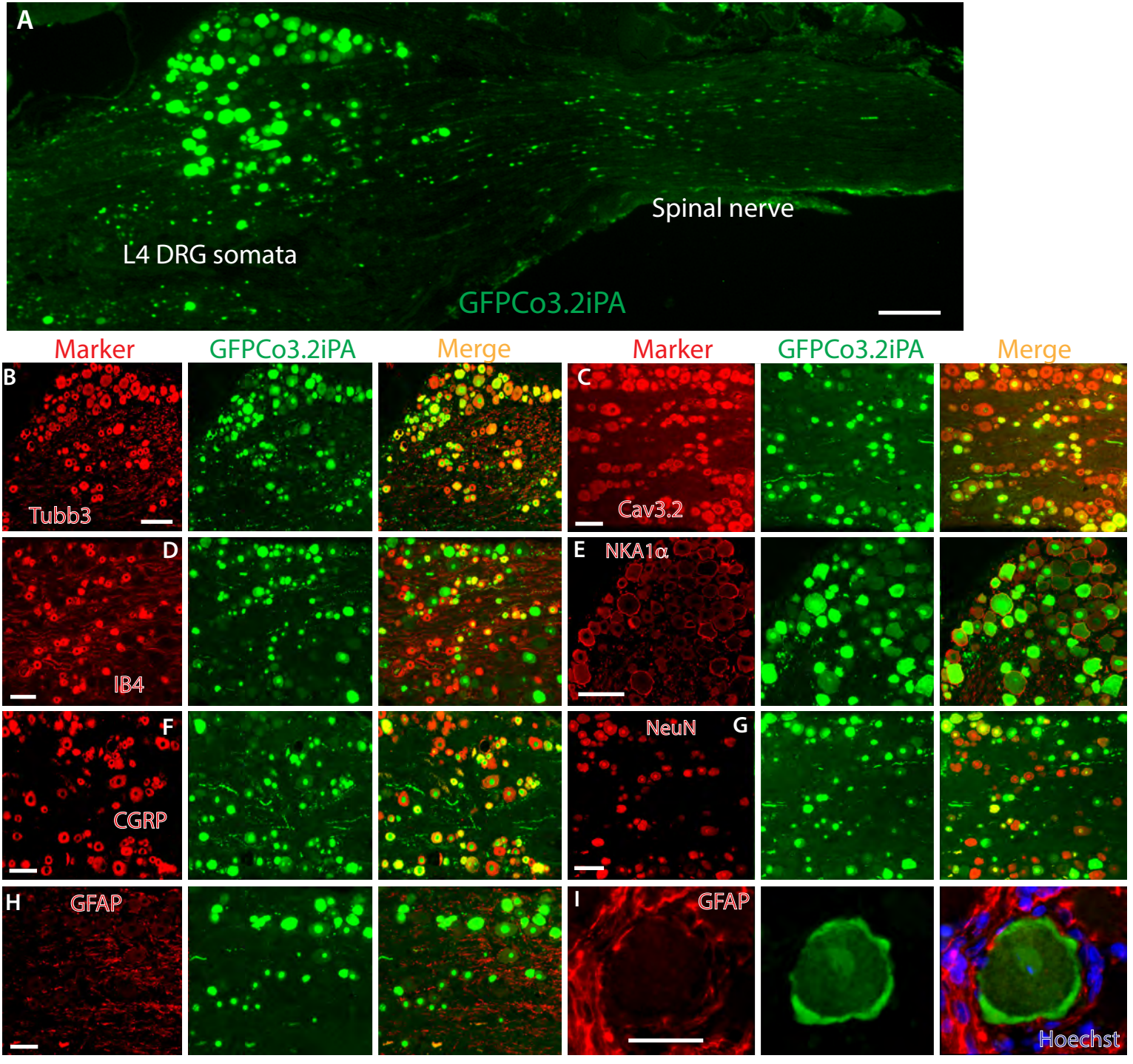

Click here to access/download;Figure (high resolution without caption);Figure 4.pdf

Figure 4

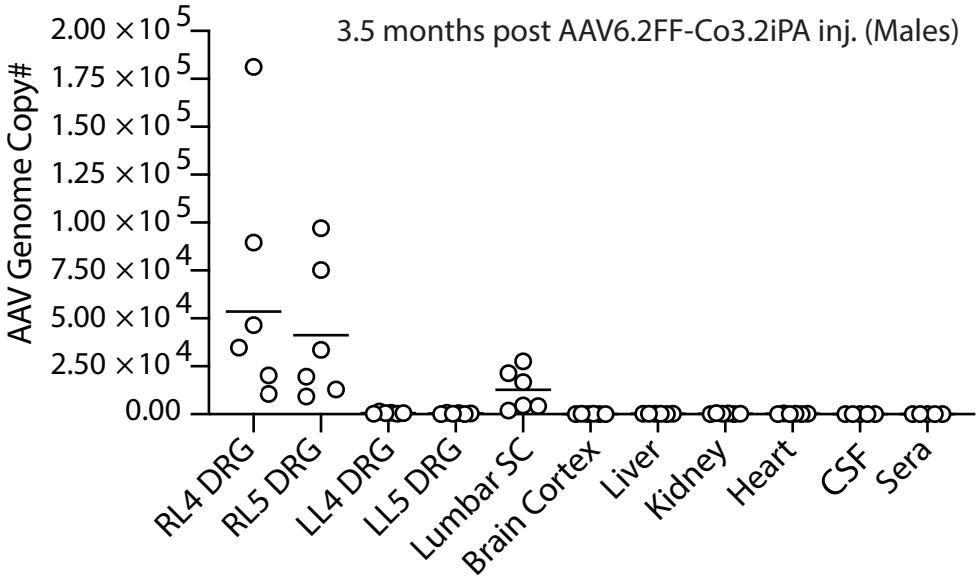

Click here to access/download;Figure (high resolution without caption);Figure 5.pdf

Figure 5

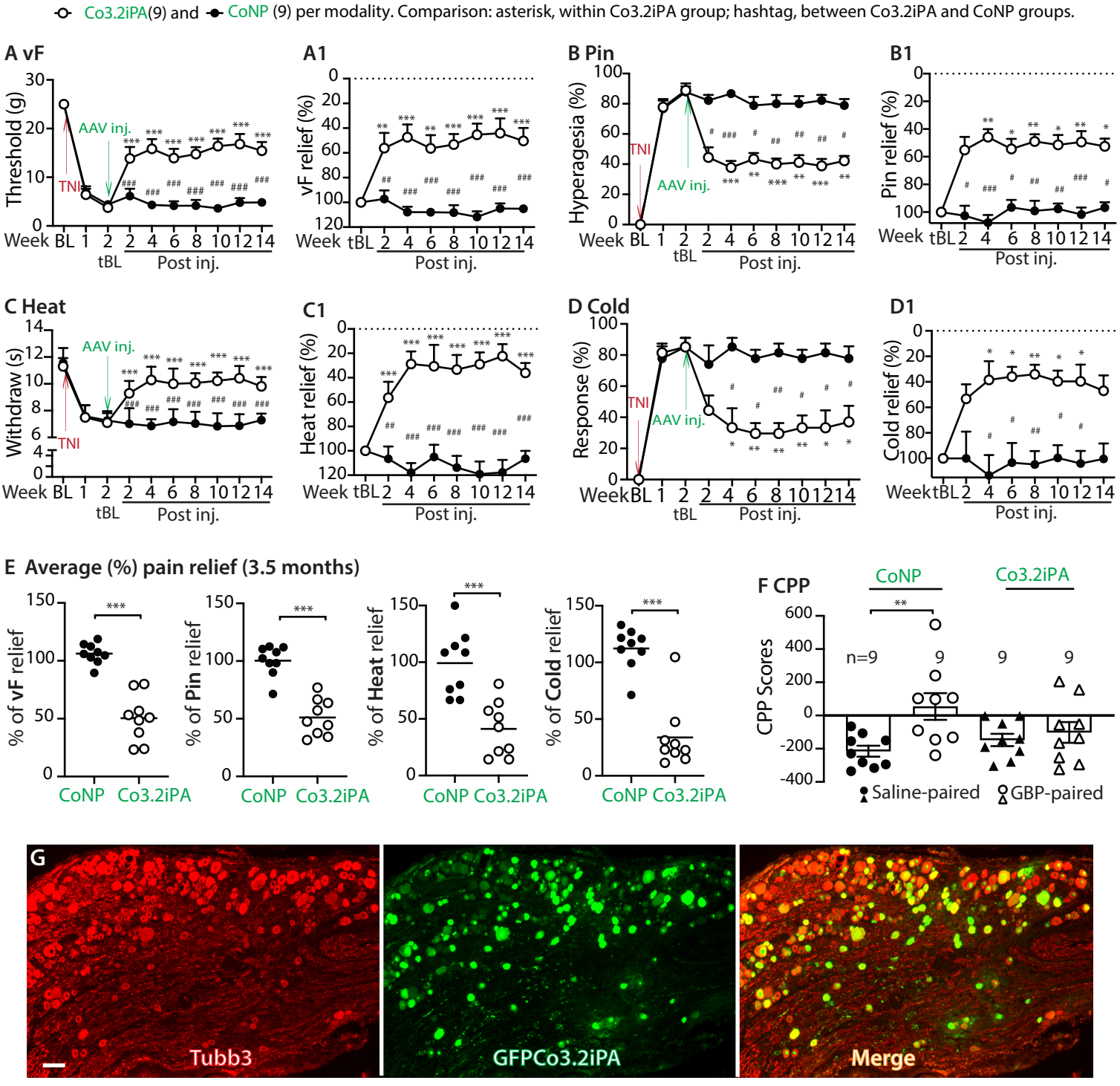

Click here to access/download;Figure (high resolution without caption);Figure 6.pdf

Figure 6

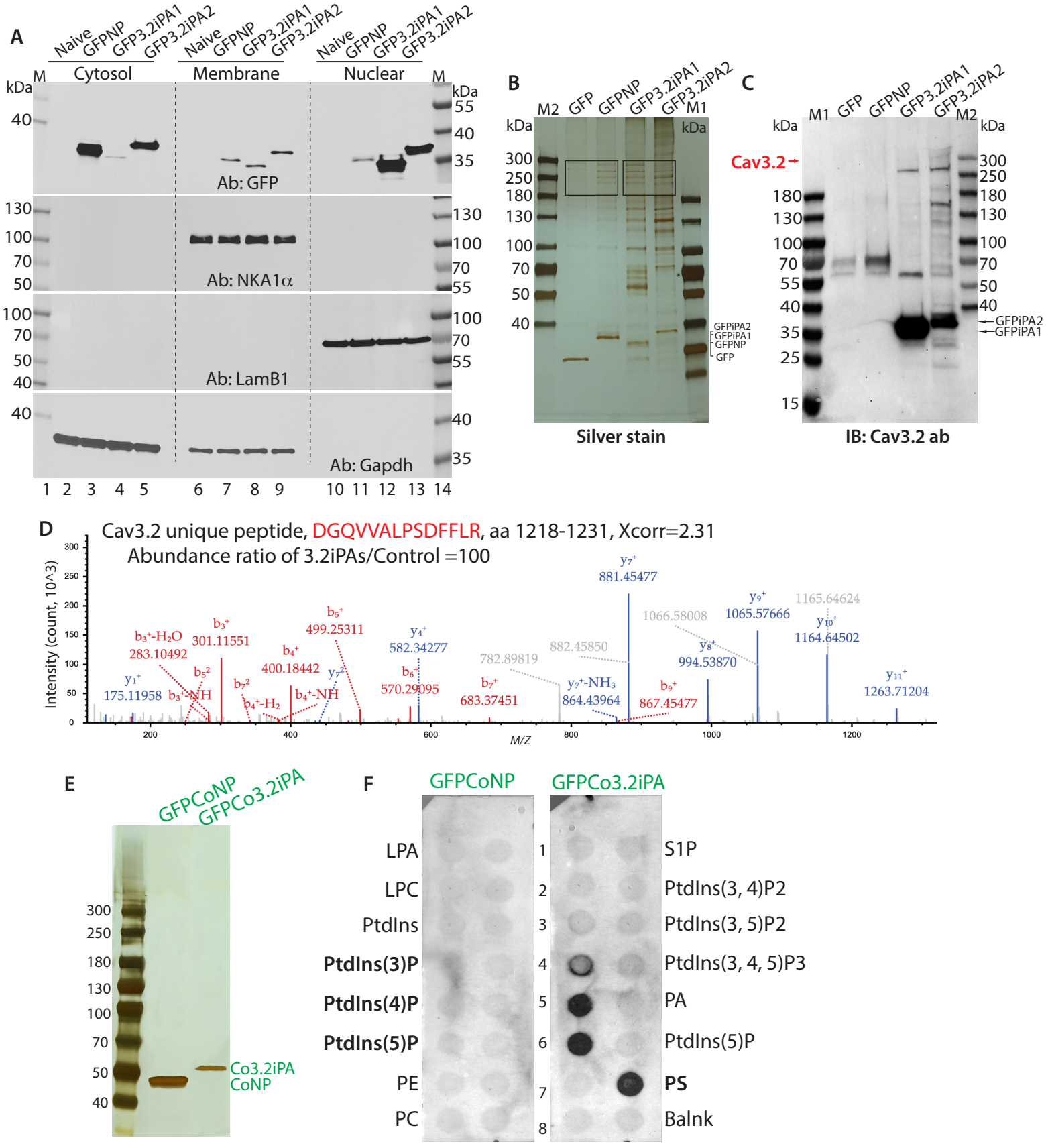

Figure 7

Click here to access/download;Figure (high resolution without caption);Figure 7.pdf

Figure 7

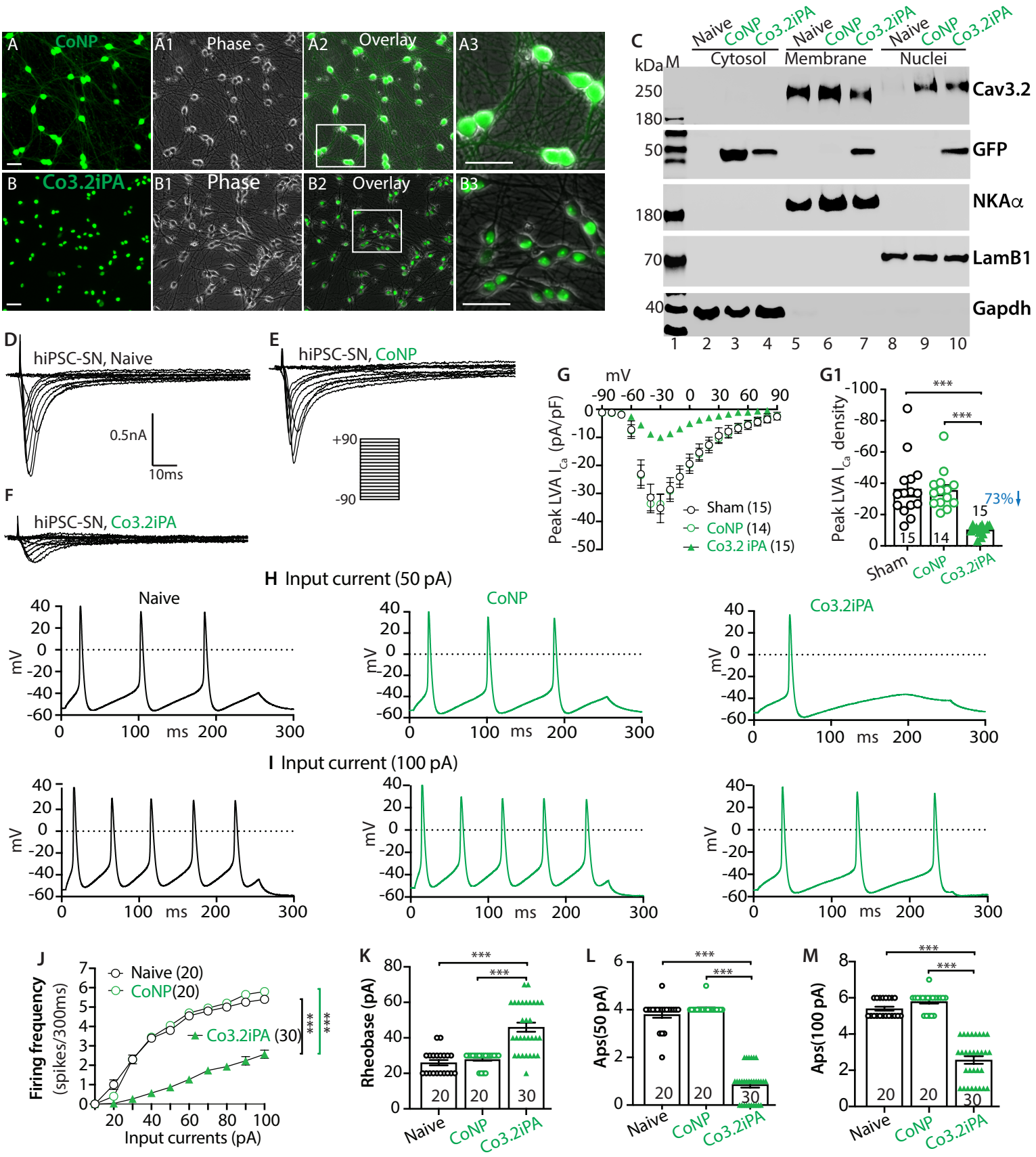

Shin et al. ***Preclinical long-lasting efficacy and translational significance of AAV-Cav3.2iPA sensory neuron-targeted analgesia for treatment of neuropathic pain***

Supplementary Materials

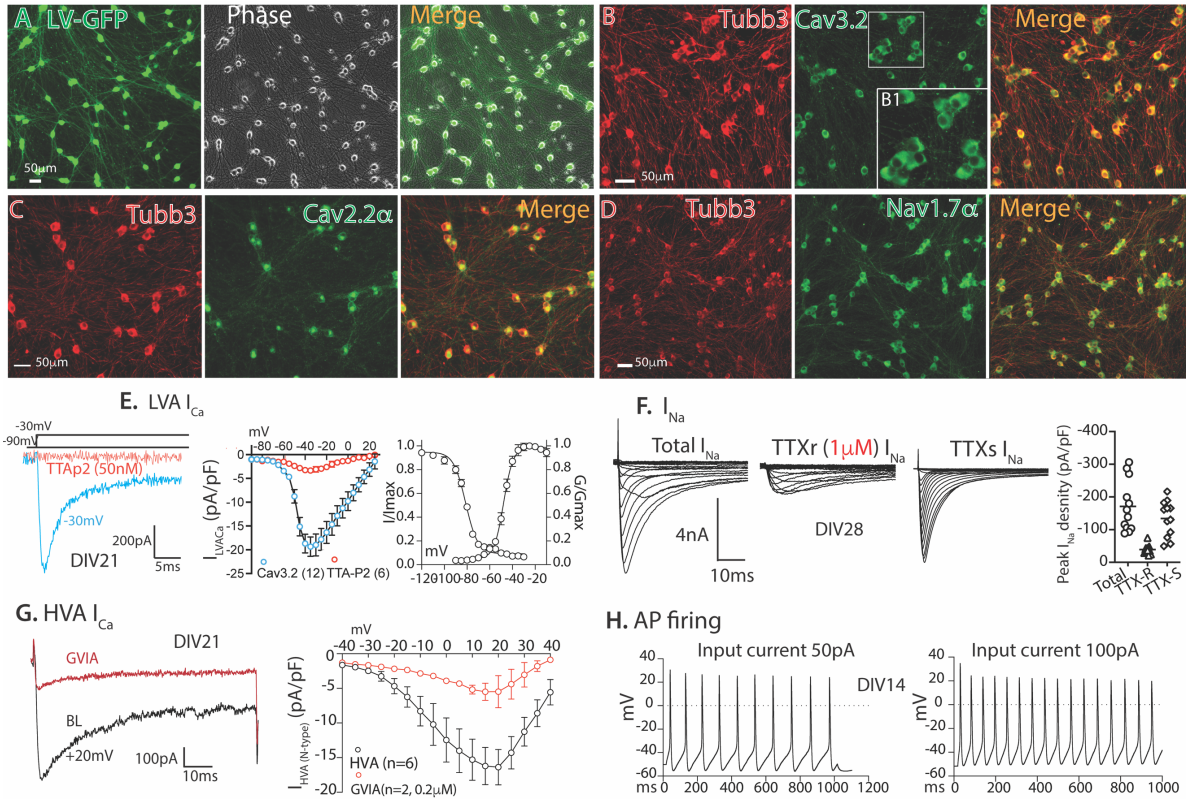

Suppl. Figure 1. HiPSC-SNs (female). (**A**) 100% transduction of hiPSC-SNs by LV-GFP (MOI=5). (**B-D**) ICC: Cav3.2, Cav3.2, and Nav1.7 (green) co-labeled with Tubb3 (red) at DIV21. Patch-clamp of T-type/Cav3.2 currents (**E**) that are sensitive to T-channel inhibitor TTAp2, (**F**) Total, TTXs, and TTXr sodium channel currents using a subtraction protocol with bath TTX (1□M) (**F**), (**G**) HVA I_{Ca}, and (**G**) AP firing, recorded from differentiated hiPSC-SN (DIV14-28). Rs is compensated at 80%

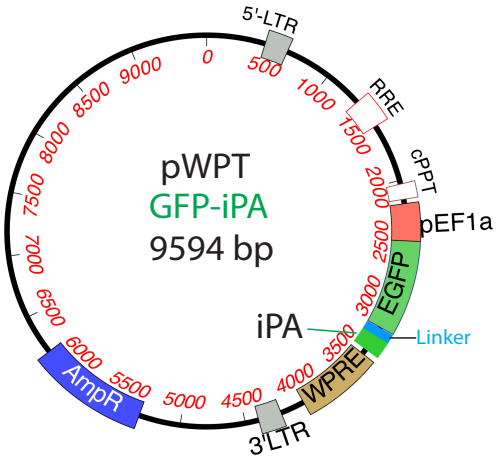

Suppl Figure 2. Construct lentivector-encoded Co3.2iPA and CoNP for hiPSC-SN transduction.

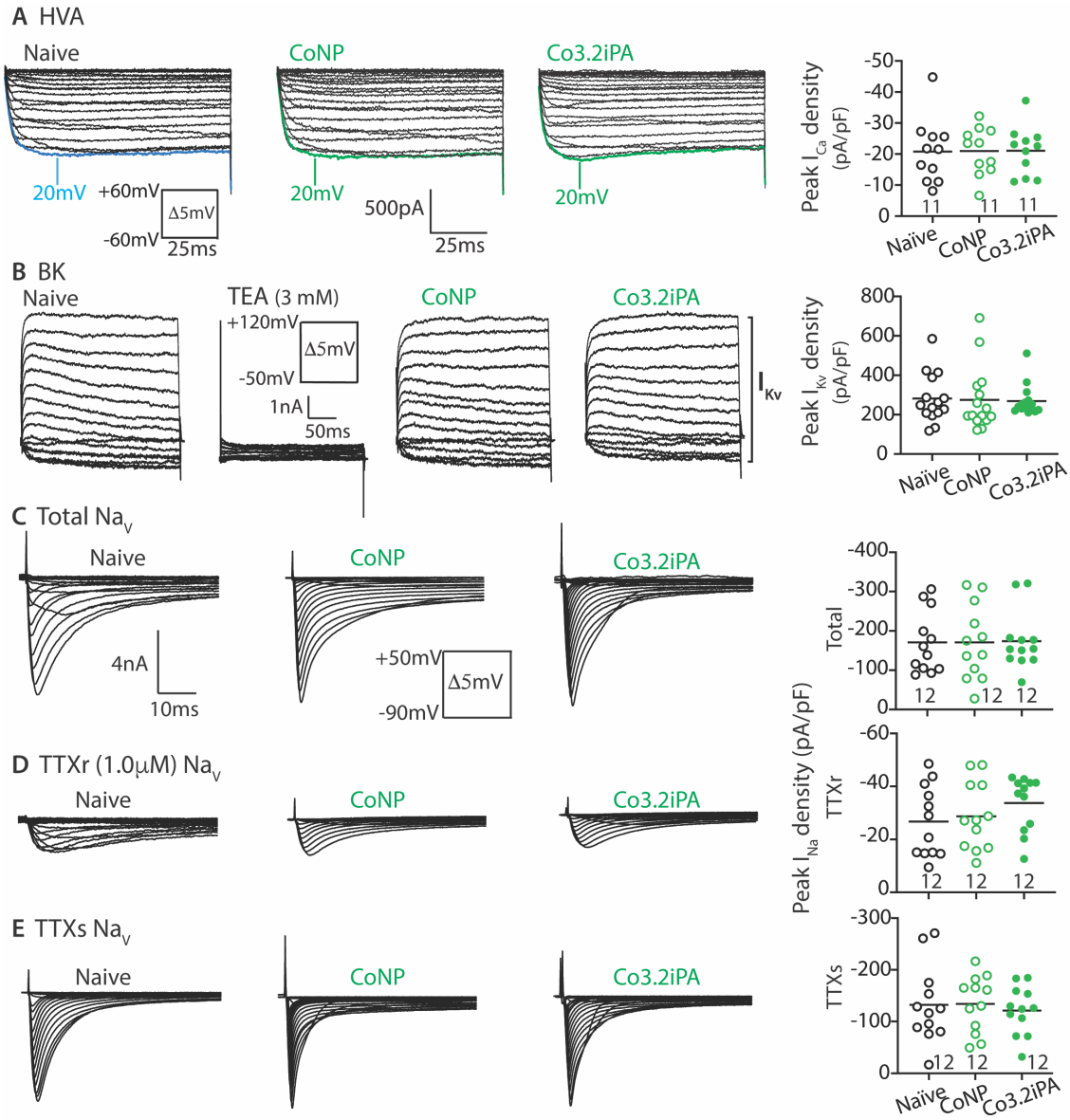

Suppl. Figure 3. Non-pleiotropic effects of Co3.2iPA expression on HVA I_{Ca}, BK I_{Kv}, and I_{Na} in hiPSC-SNs. (**A**) Representative traces of HVA I_{Ca} recorded from hiPSC-SNs (DIV21) in naïve, CoNP, and Co3.2iPA expressing hiPSC-SNs, and quantitative analysis of peak HVA I_{Ca} density (panels from left to right). One-way ANOVA and post hoc. (**B**) Representative traces of BK I_{Kv} recorded from hiPSC-SNs (DIV21) in naïve, TEA (3mM) in bath solution, CoNP, and Co3.2iPA expressing hiPSC-SNs, and quantitative analysis of peak BK I_{Kv} density (panels from left to right). One-way ANOVA and post hoc. (**C-E**) Representative traces of total I_{Na} (**C**), TTXr I_{Na} (1□M TTX in bath solution) (**D**), TTXs I_{Na} (**E**), recorded from naïve, CoNP, and Co3.2iPA expressing hiPSC-

SNs (DIV28, Inserts: pulse protocol and scales), and quantitative analysis of peak currents. A subtraction protocol is used to separate TTXr and TTXs I_{Na}.

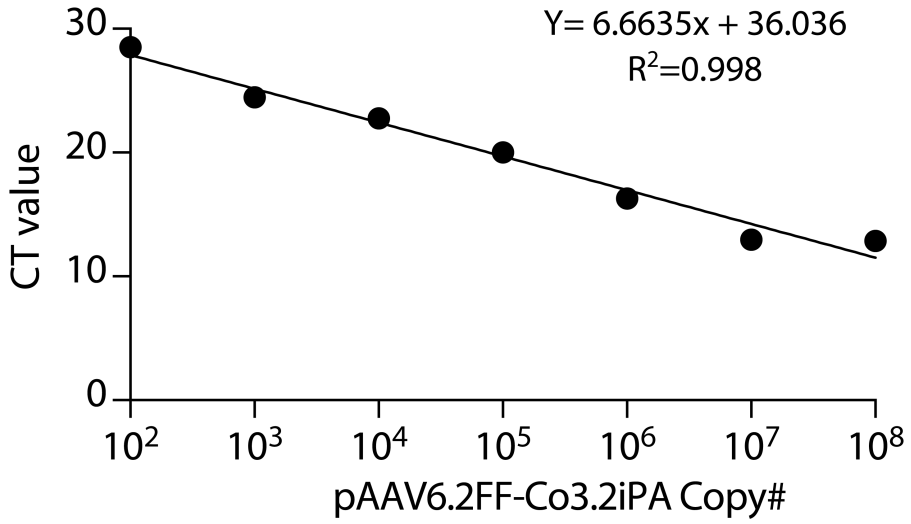

Suppl. Figure 4. QPCR standard curve of pAAV6.2FF-Co3.2iPA.

eTOC synopsis

1. AAV-mediated primary sensory neuron-specific expression Co3.2iPA inhibits T-channels and provides long-term analgesic success for neuropathic pain.
2. Inhibition of T-channel activity and action potential firing by Co3.2iPA is confirmed in human iPSC-derived sensory neurons, indicating a translational potential.

Graphic Abstract

Click here to access/download;Graphical Abstract;graphic_Abstract.tif

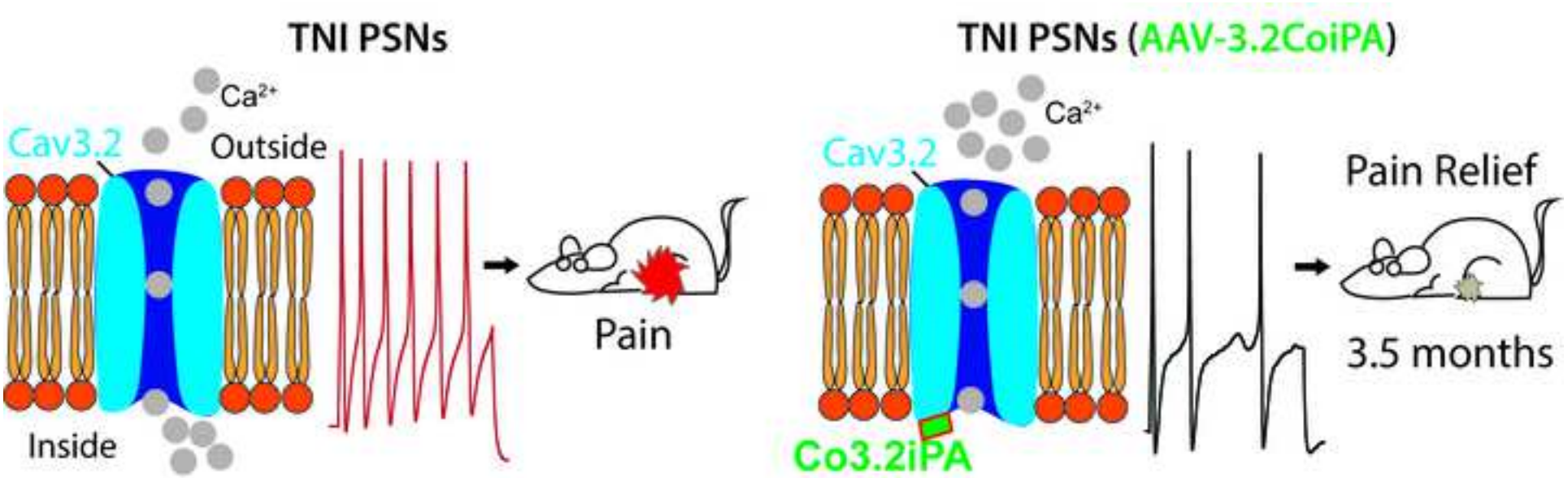

CELL PRESS DECLARATION OF INTERESTS POLICY

Transparency is essential for a reader's trust in the scientific process and for the credibility of published articles. At Cell Press, we feel that disclosure of competing interests is a critical aspect of transparency. Therefore, we require a "declaration of interests" section in which all authors disclose any financial or other interests related to the submitted work that (1) could affect or have the perception of affecting the author's objectivity or (2) could influence or have the perception of influencing the content of the article.

What types of articles does this apply to?

We require that you disclose competing interests for all submitted content by completing and submitting the form below. We also require that you include a "declaration of interests" section in the text of all articles even if there are no interests to declare.

What should I disclose?

We require that you and all authors disclose any personal financial interests (e.g., stocks or shares in companies with interests related to the submitted work or consulting fees from companies that could have interests related to the work), professional affiliations, advisory positions, board memberships (including membership on a journal's advisory board when publishing in that journal), or patent applications and/or registrations that are related to the subject matter of the contribution. As a guideline, you need to declare an interest for (1) any affiliation associated with a payment or financial benefit exceeding $10,000 p.a. or 5% ownership of a company or (2) research funding by a company with related interests. You do not need to disclose diversified mutual funds, 401ks, or investment trusts.

Authors should also disclose relevant financial interests of immediate family members. Cell Press uses the Public Health Service definition of "immediate family member," which includes spouse and dependent children.

Where do I declare competing interests?

Competing interests should be disclosed on this form as well as in a "declaration of interests" section in the manuscript. This section should include financial or other competing interests as well as affiliations that are not included in the author list. Examples of "declaration of interests" language include:

> "AUTHOR is an employee and shareholder of COMPANY."
> "AUTHOR is a founder of COMPANY and a member of its scientific advisory board."

NOTE: Primary affiliations should be included with the author list and do not need to be included in the "declaration of interests" section. Funding sources should be included in the "acknowledgments" section and also do not need to be included in the "declaration of interests" section. (A small number of front-matter article types do not include an "acknowledgments" section. For these articles, reporting of funding sources is not required.)

What if there are no competing interests to declare?

If you have no competing interests to declare, please note that in the "declaration of interests" section with the following wording:

> "The authors declare no competing interests."

April 12, 2024

CELL PRESS DECLARATION OF INTERESTS FORM

If submitting materials via Editorial Manager, please complete this form and upload with your initial submission. Otherwise, please email as an attachment to the editor handling your manuscript.

Please complete each section of the form and insert any necessary "declaration of interests" statement in the text box at the end of the form. A matching statement should be included in a "declaration of interests" section in the manuscript.

Institutional affiliations

We require that you list the current institutional affiliations of all authors, including academic, corporate, and industrial, on the title page of the manuscript. ***Please select one of the following:***

☒ All affiliations are listed on the title page of the manuscript.

☐ I or other authors have additional affiliations that we have noted in the "declaration of interests" section of the manuscript and on this form below.

Funding sources

We require that you disclose all funding sources for the research described in this work. ***Please confirm the following:***

☒ All funding sources for this study are listed in the "acknowledgments" section of the manuscript.*

*A small number of front-matter article types do not include an "acknowledgments" section. For these, reporting funding sources is not required.

Competing financial interests

We require that authors disclose any financial interests and any such interests of immediate family members, including financial holdings, professional affiliations, advisory positions, board memberships, receipt of consulting fees, etc., that:

(1) could affect or have the perception of affecting the author's objectivity, *or*
(2) could influence or have the perception of influencing the content of the article.

Please select one of the following:

☒ We, the authors and our immediate family members, have no financial interests to declare.

☐ We, the authors, have noted any financial interests in the "declaration of interests" section of the manuscript and on this form below, and we have noted interests of our immediate family members.

Advisory/management and consulting positions

We require that authors disclose any position, be it a member of a board or advisory committee or a paid consultant, that they have been involved with that is related to this study. We also require that members of our journal advisory boards disclose their position when publishing in that journal. ***Please select one of the following:***

☒ We, the authors and our immediate family members, have no positions to declare and are not members of the journal's advisory board.

☐ The authors and/or their immediate family members have management/advisory or consulting relationships noted in the "declaration of interests" section of the manuscript and on this form below.

Patents

We require that you disclose any patent applications and/or registrations related to this work by any of the authors or their institutions. ***Please select one of the following:***

☒ We, the authors and our immediate family members, have no related patent applications or registrations to declare.

☐ We, the authors, have a patent application and/or registration related to this work, which is noted in the "declaration of interests" section of the manuscript and on this form below, and we have noted the patents of immediate family members.

Please insert any "declaration of interests" statements in this space. This exact text should also be included in the "declaration of interests" section of the manuscript. If no authors have a competing interest, please insert the text, "The authors declare no competing interests."

The authors declare that the research was conducted without any commercial or financial relationships that could potentially create a conflict of interest.

☒ **On behalf of all authors, I declare that I have disclosed all competing interests related to this work. If any exist, they have been included in the "declaration of interests" section of the manuscript.**